https://doi.org/10.1016/j.trb.2020.12.006

This is the Pre-Published Version.

# A joint liner ship path, speed and deployment problem under emission reduction measures

Dan Zhuge[a,b], Shuaian Wang[b], David Z.W. Wang[a,*]

[a] *School of Civil and Environmental Engineering, Nanyang Technological University, 50 Nanyang Avenue, Singapore 639798, Singapore*
[b] *Department of Logistics & Maritime Studies, The Hong Kong Polytechnic University, Hung Hom, Hong Kong, China*

## Abstract

This paper addresses a joint ship path, speed, and deployment problem in a liner shipping company considering three emission reduction measures, including sulfur emission regulations, carbon tax, and vessel speed reduction incentive programs (VSRIPs). Given a set of service routes and the total number of available ships, the proposed problem determines how many ships should be deployed on each route and how to design sailing path and speed for each leg. A mixed-integer non-linear programming model is presented for minimizing the total cost of all routes, i.e., fuel cost, carbon tax, and fixed cost, minus dockage refund. The different impacts of the three emission reduction measures on sailing path and speed complicate the problem. Some important properties are obtained by analyzing the proposed model. Combining these properties with a dynamic programming approach, a tailored method is developed to solve the problem. Based on real data, extensive numerical experiments are conducted to examine the validity of the proposed model and the efficiency of the solution method. The computational results demonstrate that the proposed model can contribute to significant cost savings for shipping companies.

*Keywords:* Path and speed optimization; fleet deployment; dynamic programming; sulfur emission regulations; carbon tax; vessel speed reduction incentive program (VSRIP)

## 1. Introduction

The shipping industry plays a central role in international trade. UNCTAD (2019) reported that the international maritime trade increased from 7,702 million tons in 2006 to 11,005 million tons in 2018 (see Fig. 1), and its growth rate was expected to be 2.6% in 2019. It is evident that, without regulations, the international maritime trade will lead to

[*] Corresponding author. wangzhiwei@ntu.edu.sg (David Z.W. Wang)

© 2020. This manuscript version is made available under the CC-BY-NC-ND 4.0 license https://creativecommons.org/licenses/by-nc-nd/4.0/

considerable shipping emissions, including sulfur dioxide ($SO_2$), nitrogen oxides ($NO_x$), carbon dioxide ($CO_2$), and particulate matter (PM). Recently, air emissions generated by frequent shipping activities have caused serious environmental and health problems (Cullinane and Edwards, 2010; Kirschstein and Meisel, 2015). A report by Sofiev et al. (2018) even showed that shipping emissions indirectly contribute to at least 400,000 premature deaths per year globally. It is important for the government, academia and industry to pay more attention to ship emissions considering the severity of the problem.

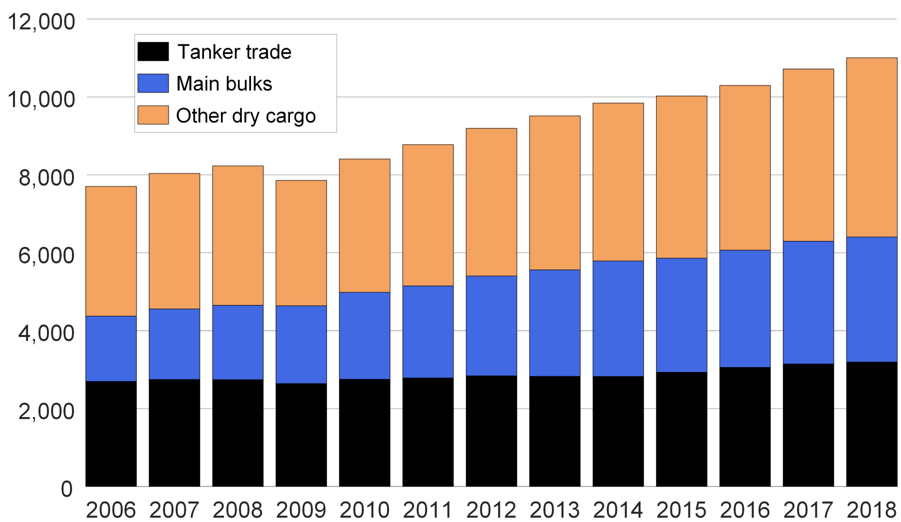


Figure 1: International maritime trade (Million tons loaded)

Notes:
(i) "Tanker trade" includes crude oil, refined petroleum products, gas and chemicals.
(ii) "Main bulks" include iron ore, grain and coal.
(iii) "Other dry cargo" includes minor bulks, containerized trade and residual general cargo.

Quite a number of emission reduction measures and policies have been presented in the shipping industry. Four international emission control areas (ECAs), i.e., the Baltic Sea area, the North Sea area, the North America area, and the United States Caribbean Sea area, have been established, and marine bunker fuels with higher than 0.1% sulfur content are prohibited in these four areas since 1 January 2015. The establishment of ECAs is effective in sulfur emission reduction near the coast (Browning et al., 2012; Chang et al., 2014; Svindland, 2018; Zhang et al., 2020), and it may also have an effect on the sailing pattern of ships. As pointed out by Doudnikoff and Lacoste (2014), Fagerholt et al. (2015), Fagerholt and Psaraftis (2015), Gu and Wallace (2017), Chen et al. (2018), and Zhen et al. (2020a), the ECAs will lead to the differentiated speeds within and outside ECAs and the detour of sailing paths, which would result in increased total emissions, while Adland et al. (2017) and Fan and Huang (2019) reported that the ECA regulation may not cause the change of sailing speeds. The effects of different factors on sailing pattern and evasion strategy in the context of sulfur emission regulations have been discussed by Li et al. (2020). In order to further reduce $SO_2$ emissions from ships worldwide, the 0.5% global sulfur limit has been put into force from 1 January 2020. Marine gas oil (MGO) with at most 0.1% sulfur content can be used within ECAs, and very low-sulfur fuel oil (VLSFO) with the sulfur content no more than 0.5% is widely applied outside ECAs. According to the global average bunker fuel price in the first three months of 2020, the price of MGO is around 20% higher than that of VLSFO and 80% higher than that of heavy fuel oil (HFO) with at most 3.5% sulfur content, and thus the lower price gap between the fuel used within ECAs and that outside after the implementation of 0.5% global sulfur limit may contribute to the mitigation of detour issue, while this problem will still exist due to the price difference between MGO and VLSFO (Li et al., 2020).

Considerable greenhouse gas (GHG) emissions annually generated by the maritime activity are another focus in recent years, which account for 2.5% of the total amount (IMO, 2014). The International Maritime Organization (IMO) has proposed an initial strategy for reducing GHG emissions in the shipping industry to mitigate the threat of climate change. This strategy aims to reduce $CO_2$ emissions by at least 40% by 2030 compared with the level in 2008. Carbon tax that directly fixes a price for $CO_2$ emission is a significantly economical means for GHG reduction. As one of the market-based measures, its introduction in the proposed strategy has been discussed for a number of years (UNCTAD, 2019). Recently, the European Parliament has voted to include maritime transportation in EU emissions trading system (Lloyd's List, 2020). The effectiveness of the carbon tax policy in the shipping industry has been validated by Kim et al. (2012) and Wang and Xu (2015).

While both sulfur emission regulations and carbon tax will affect the global emissions, a vessel speed reduction incentive program (VSRIP) adopted at port of Los Angeles (LA) only focuses on the emissions near ports. In the VSRIP of LA, two vessel speed reduction zones (VSRZs) with the radii of 20 and 40 nautical miles (nm) are designed, and the speed limits in both VSRZs are 12 nm/hour (knots). Ships complying with the speed requirement in 20 nm VSRZ and 40 nm VSRZ can obtain 15% and 30% refunds of their first day dockage, respectively. Although the VSRIP is a voluntary program, most of the ships that visit LA have participated in it partly because of the dockage refund (Ahl et al., 2017), and the participation rate in 2019 was 91%. Similar programs have also been implemented at ports of Long Beach, San Diego, and New York and New Jersey and several major ports in South Korea. Considering that the fuel consumption can be calculated by an approximately cubic function of sailing speed (Corbett et al., 2009; Wang and Meng, 2012; Koza, 2019), slow steaming can contribute to the emission reduction of all exhaust gases and particulates. The adoption of VSRZs as well as its positive effect on shipping emission reduction has been further discussed and confirmed by Khan et al. (2012), Chang and Wang (2014), Zis et al. (2014), Zis (2015), Chang and Jhang (2016), and López-Aparicio et al. (2017).

Extensive recent studies have focused on ship routing, schedule design, and fleet deployment, such as Andersson et al. (2015), Karsten et al. (2018), Ng and Lin (2018), Tan et al. (2018), Ng (2019), Wang et al. (2019), Zhen et al. (2019), Dong et al. (2020a), and Dong et al. (2020b), most of which can also been seen in the surveys, including Meng et al. (2014), Wang and Meng (2017), and Zis et al. (2020). Further, many research works on the shipping network design problem take into account one or two of the three emission reduction measures, i.e., sulfur emission regulations (Cariou et al., 2018; Zhen et al., 2018; Sheng et al., 2019; Zhao et al., 2019; Ma et al., 2020a,b; Reinhardt et al., 2020; Zhen et al., 2020b), carbon tax (Wang and Chen, 2017; Xin et al., 2019), and VSRIPs (Zhuge et al., 2020). Traditional ships complying with sulfur emission regulations may lower sailing speed within ECAs and choose a path with a shorter distance within ECAs to reduce the use of expensive 0.1% low-sulfur fuel; ships complying with the speed limits in the VSRIPs can obtain financial incentives. Carbon tax is expected to have a different impact on sailing path and speed. However, no previous research works in the existing literature have ever focused on the shipping network optimization problem under all of the three measures. To fill this research gap, our study investigates how to find the optimal operation strategies on the sailing speeds and path of each leg, the number of ships deployed on each route and the compliance of each VSRZ for a shipping company that operates a fixed fleet of traditional ships on its existing liner routes, considering sulfur emission regulations, carbon tax, and VSRIPs. The fixed cost of a route depends on the number of ships deployed on the route. Due to the weekly service frequency provided by the company, when more ships are deployed, its rotation time will be longer, the average sailing speed will be lower, and the fuel consumption, the fuel cost and $CO_2$ emissions will also be lower. Therefore, the fleet deployment problem for all routes needs to balance fixed cost, fuel cost and carbon tax.

Focusing on one route with a given number of ships deployed, the fixed cost is constant, and we will minimize the cost of the route, including fuel cost and carbon tax minus dockage refund, by optimizing the sailing speeds and choosing the path for each leg, as well as deciding the compliance of VSRZs at each port. The traditional ships should use 0.1% lower-sulfur fuel within ECAs and 0.5% lower-sulfur fuel outside. Participating in a VSRIP means ships should comply with the speed limit in the program. As a result, differentiated speeds may be designed for the sailing within only ECAs, within only VSRZs [1], within both ECAs and VSRZs, and outside both ECAs and VSRZs on each leg. As the leg covering ECAs has infinite sailing paths, to make the problem more tractable, a set of feasible paths will be designed for the leg by discretizing the ECA boundaries. The interactive decisions on the sailing speeds and path, and the compliance of VSRZs complicate the optimization problem for each route. We find some properties on this liner ship path, speed, and deployment problem. On the basis of these properties and dynamic programming approach, a tailored algorithm is developed to address the studied problem with the aim of minimizing the total cost of all routes, consisting of fuel cost, carbon tax, and fixed cost, minus dockage refund.

The main contributions of this study are fourfold. Firstly, this study is the first to address the joint ship path, speed, and deployment problem of a liner shipping company under three important emission reduction measures (i.e., sulfur emission regulations, carbon tax, and VSRIPs) and investigate the effects of the three measures on liner ship service planning. Secondly, we obtain some interesting findings on the proposed model, including the propositions regarding the choice of sailing path, the compliance of VSRZs, and the property of the total cost function for each route. Thirdly, based on some properties derived and dynamic programming, a tailored solution algorithm is developed, whose solution efficiency is validated by extensive numerical experiments. Lastly, the research outcome of this study is able to assist the shipping service operators in making a better decision on how to design the number of ships deployed on each route, the sailing path for each leg, and the sailing speeds within only ECAs, within only VSRZs, within both ECAs and VSRZs, and outside both ECAs and VSRZs under the three measures, which would result in a significant amount of operating cost savings for the shipping company. As shipping lines are still suffering from the deep effects from the financial

[1] For brevity, we use the term "within only ECAs" to refer to the case within ECAs and outside VSRZs and the term "within only VSRZs" to refer to the case within VSRZs and outside ECAs.

crisis of 2008 and international trade has plummeted due to the outbreak of COVID-19 and Sino-US friction, it is crucial for the operators to reduce the increased cost incurred by compulsory emission reduction measures.

The remainder of the paper is organized as follows. Section 2 elaborates the joint liner ship path, speed, and deployment problem and builds a mixed-integer non-linear mathematical model. Some properties of the model is obtained, and then a tailored algorithm based on dynamic programming is developed in Section 3. Section 4 conducts a large number of numerical experiments. Finally, conclusions are outlined in the last section.

## 2. Model formulation

We will analyze a joint problem on sailing path, sailing speed, and fleet deployment in a liner shipping line considering sulfur emission regulations, carbon tax, and VSRIPs simultaneously. The liner shipping company operates $Q$ traditional ships with the maximum speed $V^{\max}$, which need to use 0.1% low-sulfur fuel within ECAs and 0.5% low-sulfur fuel outside ECAs. These ships can be deployed on the routes defined in the set $R$ and a route $r \in R$ provides a weekly service frequency whose legs are defined in the set $I_r$. A leg $i \in I_r$ is a sailing from a port of call to the next. We consider four types of ports in our study, including ports located within ECAs and without any VSRZ (defined as ECA ports), ports outside ECAs and with VSRZs (defined as VSRZ ports), ports within ECAs and with VSRZs (defined as ES ports), and ports outside ECAs and without VSRZs (defined as non-ES ports).

To generalize the problem, a VSRIP at a port $p$ called on route $r$ can have several VSRZs with different radii in our study, denoted by the set $J_{rp}$. These VSRZs are recorded as VSRZ 1, 2, ..., $|J_{rp}|$ in the increasing order of radius. Based on the existing ECAs and VSRIPs, we assume that the longest radius of VSRZs will be shorter than the distance from the ECA boundary to a port. VSRZ 0, only defined at VSRZ or ES ports, means ships do not participate in the VSRIP. A VSRZ whose speed limit is complied with is called chosen VSRZ, and VSRZ 0 also can be regarded as the chosen VSRZ when the speed limit in the VSRIP has not been obeyed. The speed limit in all VSRZs is 12 knots, denoted by $V^S$. A VSRZ in a VSRIP with a longer radius than another in the same program provides higher dockage refund, and the dockage refunds vary in different VSRIPs. Each ship visit can obtain a dockage refund from only one VSRZ at a VSRZ or ES port by participating in its VSRIP. If a VSRZ or ES port is called several times on a route, ships participating in the VSRIP can receive a refund by each visit, and these ports of call are regarded as different ports in our study. We construct some VSRZ groups for each route with VSRZ or ES ports. A VSRZ group consists of several VSRZs at different VSRZ and ES ports, where the sum of radii of all VSRZs at ES ports in the group is recorded as ES distance and that at VSRZ ports is VSRZ distance. For example, a VSRZ group with the ES distance of 60 nm can be composed of three 20 nm VSRZs or one 20 nm VSRZ and one 40 nm VSRZ at ES ports.

Recall that the ECA may lead to the detour of ships because of the stricter sulfur limit within the area and the different distance from each ECA boundary point to the port; hereby, as the radius of VSRZ, i.e., the distance from each VSRZ boundary point to the port, is constant, no detour will be caused by the VSRZ. As shown in Fig. 2, a trajectory from port A to detour point C on the ECA boundary and then from point C to port B is defined as a sailing path of the leg from port A to port B. A leg covering

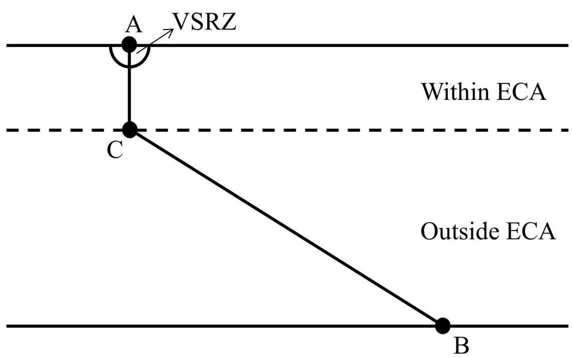


Figure 2: A path illustration

ECAs and/or chosen VSRZs will be divided into several stretches by the ECA boundaries and/or the chosen VSRZ boundaries. A stretch refers to a sailing with different ECA and VSRZ implementation situations, that is a sailing within only the ECA, within only the chosen VSRZ, within both the ECA and the chosen VSRZ near a port of a leg, or a sailing outside both ECAs and chosen VSRZs on a leg. Considering that the radius of VSRZ is always shorter than the distance from the coast to the ECA boundary, the number of stretches on each type of leg is schematically illustrated in Fig. 3. For a leg $i$ of route $r$, its stretches within only ECAs, within only chosen VSRZs, within both ECAs and chosen VSRZs, and outside both ECAs and chosen VSRZs define the sets $M_{ri}^{E}$, $M_{ri}^{S}$, $M_{ri}^{ES}$, and

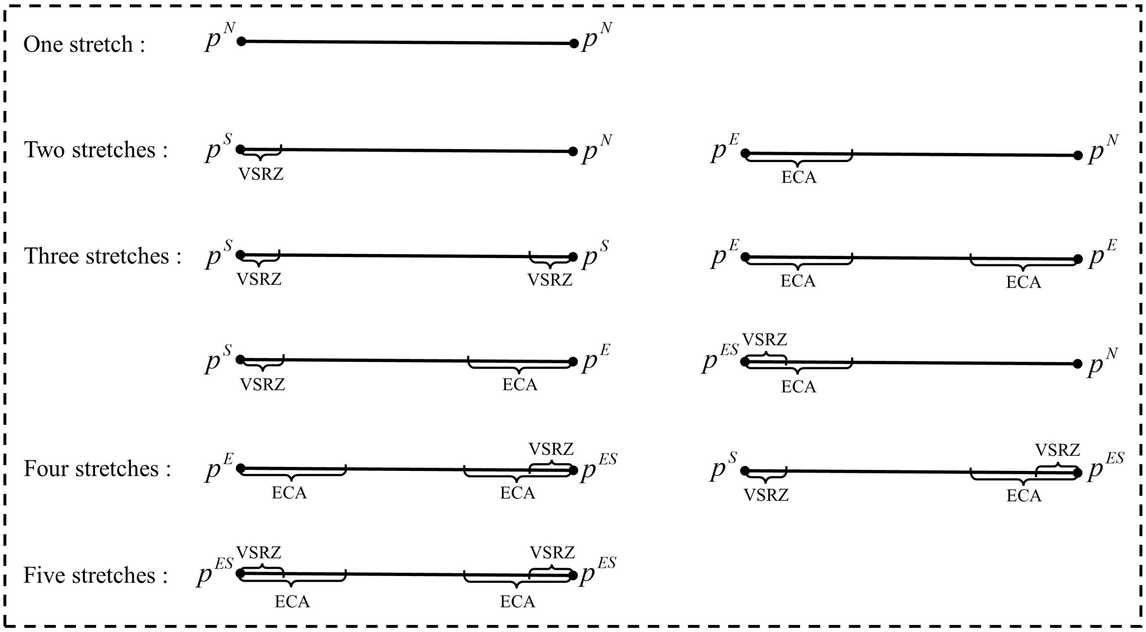


Figure 3: Number of stretches for different types of legs

Notes: "$p^N$" denotes the non-ES port, "$p^E$" denotes the ECA port, "$p^S$" denotes the VSRZ port, and "$p^{ES}$" denotes the ES port.

$M_{ri}^N$, respectively. Differentiated speeds may be designed on different stretches of a leg covering ECAs and/or VSRZs for saving 0.1% low-sulfur fuel and obtaining the dockage refund. Considering the approximately cubic relationship between sailing speed and fuel consumption, ships should sail at the average speed on a stretch, and further, the speeds on the stretches within only ECAs of a leg should be the same in the optimal solution.

The carbon tax is designed by the price of $CO_2$ in European carbon trading market. The same amount of $CO_2$ emissions will be generated from one ton of 0.1% or 0.5% low-sulfur fuel consumption, and the introduction of carbon tax may lead to the change of sailing network design in the company. Under the three measures, a mixed-integer non-linear programming model with the aim of minimizing the total cost, including fuel cost, carbon tax, and fixed cost, minus dockage refund, will be proposed to optimize fleet deployment, sailing path and speeds, and compliance of VSRIPs. We first provide the notation frequently used in the model.

**Sets**

| | |
|---|---|
| $R$ | Set of routes |
| $I_r$ | Set of legs on route $r \in R$ |
| $M_{ri}^E$ | Set of stretches within only ECAs on leg $i \in I_r$ of route $r \in R$ |
| $M_{ri}^S$ | Set of stretches within only chosen VSRZs on leg $i \in I_r$ of route $r \in R$ |
| $M_{ri}^{ES}$ | Set of stretches within both ECAs and chosen VSRZs on leg $i \in I_r$ of route $r \in R$ |
| $M_{ri}^N$ | Set of stretches outside both ECAs and chosen VSRZs on leg $i \in I_r$ of route $r \in R$ |
| $M_{ri}$ | Set of stretches on leg $i \in I_r$ of route $r \in R$; $M_{ri} = M_{ri}^E \cup M_{ri}^S \cup M_{ri}^{ES} \cup M_{ri}^N$ |
| $K_{ri}$ | Set of sailing paths on leg $i \in I_r$ of route $r \in R$ |
| $L_r$ | Set of super paths for route $r \in R$ obtained by Algorithm 1, where a super path of route $r \in R$ is the path combination for all the legs of the route |
| $P_r^S$ | Set of VSRZ ports on route $r \in R$ |
| $P_r^{ES}$ | Set of ES ports on route $r \in R$ |
| $J_{rp}$ | Set of VSRZs at port $p \in P_r^S \cup P_r^{ES}$ of route $r \in R$; VSRZ $0 \in J_{rp}$ means the speed limit of the VSRIP at port $p \in P_r^S \cup P_r^{ES}$ of route $r \in R$ has not been obeyed |

**Parameters**

| | |
|---|---|
| $\alpha_{rim}$ | Unit price of fuel used on stretch $m \in M_{ri}$ of leg $i \in I_r$ for route $r \in R$; $\alpha_{rim}$ equals the unit price of fuel with 0.1% sulfur (denoted by $\alpha^E$) if $m$ belongs to $M_{ri}^E \cup M_{ri}^{ES}$, and $\alpha_{rim}$ equals the unit price of fuel with 0.5% sulfur (denoted by $\alpha^N$) if $m$ belongs to $M_{ri}^S \cup M_{ri}^N$ |
| $a, b$ | Conversion factors between fuel consumption per unit distance and sailing speed; fuel consumption per unit distance of a ship is $a \cdot speed^b$ (knots), where $a > 0$ and $b > 1$ |
| $c^{CO_2}$ | Carbon tax caused by consuming one ton of fuel |
| $c^{fix}$ | Fixed cost of a ship per week |
| $c_{rpj}^{ref}$ | Dockage refund for a ship visit by complying with the speed limit in VSRZ $j \in J_{rp}$ of port $p \in P_r^S \cup P_r^{ES}$ for route $r \in R$ |
| $d_{rik}^E$ | Sailing distance within ECAs for path $k \in K_{ri}$ of leg $i \in I_r$ on route $r \in R$ |
| $d_{rik}^N$ | Sailing distance outside ECAs for path $k \in K_{ri}$ of leg $i \in I_r$ on route $r \in R$ |
| $d_{rl}^E$ | Sailing distance within ECAs for super path $l \in L_r$ of route $r \in R$ |

$d_{rl}^{N}$ Sailing distance outside ECAs for super path $l \in L_r$ of route $r \in R$

$d_{rpj}$ Radius of VSRZ $j \in J_{rp}$ at port $p \in P_r^S \cup P_r^{ES}$ of route $r \in R$

$p_{rim}^{S}$ VSRZ port on stretch $m \in M_{ri}^{S}$ of leg $i \in I_r$ for route $r \in R$

$p_{rim}^{ES}$ ES port on stretch $m \in M_{ri}^{ES}$ of leg $i \in I_r$ for route $r \in R$

$V_{rim}$ Speed limit on stretch $m \in M_{ri}$ of leg $i \in I_r$ for route $r \in R$; $V_{rim}$ equals the maximum physical speed for ships (denoted by $V^{\max}$) if $m$ belongs to $M_{ri}^{E} \cup M_{ri}^{N}$, and $V_{rim}$ equals the upper speed limit in VSRZs (denoted by $V^S$) if $m$ belongs to $M_{ri}^{S} \cup M_{ri}^{ES}$

$Q$ Total number of ships in the shipping company

$T$ Hours in a week; $T = 168h$

$T_r$ Total port time on route $r \in R$

**Variables**

$q_r$ Number of ships deployed on route $r \in R$

$t_{rim}$ Sailing time on stretch $m \in M_{ri}$ of leg $i \in I_r$ for route $r \in R$

$x_{rim}$ Sailing distance on stretch $m \in M_{ri}$ of leg $i \in I_r$ for route $r \in R$

$y_{rpj}$ Binary variable, equal to one if the speed limit for VSRZ $j \in J_{rp}$ at port $p \in P_r^S \cup P_r^{ES}$ of route $r \in R$ is obeyed, and zero otherwise

$z_{rik}$ Binary variable, equal to one if path $k \in K_{ri}$ on leg $i \in I_r$ of route $r \in R$ is chosen, and zero otherwise

The proposed problem is then formulated as:

$$[\mathbb{P}] \quad \min \sum_{r \in R} \sum_{i \in I_r} \sum_{m \in M_{ri}} (\alpha_{rim} + c^{CO_2}) x_{rim} \cdot a\left(\frac{x_{rim}}{t_{rim}}\right)^b + \sum_{r \in R} c^{fix} \cdot q_r - \sum_{r \in R} \sum_{p \in P_r^S \cup P_r^{ES}} \sum_{j \in J_{rp}} c_{rpj}^{ref} \cdot y_{rpj} \quad (1)$$

subject to

$$\sum_{i \in I_r} \sum_{m \in M_{ri}} t_{rim} = T \cdot q_r - T_r, \forall r \in R \quad (2)$$

$$\sum_{r \in R} q_r \leq Q \quad (3)$$

$$\sum_{m \in M_{ri}^{E} \cup M_{ri}^{ES}} x_{rim} = \sum_{k \in K_{ri}} d_{rik}^{E} \cdot z_{rik}, \forall r \in R, \forall i \in I_r \quad (4)$$

$$\sum_{m \in M_{ri}^{S} \cup M_{ri}^{N}} x_{rim} = \sum_{k \in K_{ri}} d_{rik}^{N} \cdot z_{rik}, \forall r \in R, \forall i \in I_r \quad (5)$$

$$\sum_{k \in K_{ri}} z_{rik} = 1, \forall r \in R, \forall i \in I_r \tag{6}$$

$$x_{rim} = \sum_{j \in J_{rp}} d_{rpj} \cdot y_{rpj}, \forall r \in R, \forall i \in I_r, \forall m \in M_{ri}^{S}, p = p_{rim}^{S} \tag{7}$$

$$x_{rim} = \sum_{j \in J_{rp}} d_{rpj} \cdot y_{rpj}, \forall r \in R, \forall i \in I_r, \forall m \in M_{ri}^{ES}, p = p_{rim}^{ES} \tag{8}$$

$$\sum_{j \in J_{rp}} y_{rpj} = 1, \forall r \in R, \forall p \in P_r^S \cup P_r^{ES} \tag{9}$$

$$x_{rim} \leq V_{rim} \cdot t_{rim}, \forall r \in R, \forall i \in I_r, \forall m \in M_{ri} \tag{10}$$

$$q_r \in \mathbb{N}, \forall r \in R \tag{11}$$

$$t_{rim} \geq 0, \forall r \in R, \forall i \in I_r, \forall m \in M_{ri} \tag{12}$$

$$x_{rim} \geq 0, \forall r \in R, \forall i \in I_r, \forall m \in M_{ri} \tag{13}$$

$$y_{rpj} \in \{0, 1\}, \forall r \in R, \forall p \in P_r^S \cup P_r^{ES}, \forall j \in J_{rp} \tag{14}$$

$$z_{rik} \in \{0, 1\}, \forall r \in R, \forall i \in I_r, \forall k \in K_{ri}. \tag{15}$$

There are three terms in the objective function of Model [$\mathbb{P}$]. The first term is the fuel cost and carbon tax for all stretches. We define $0/0 = 0$ when $t_{rim} = 0$ for all $r \in R$, $i \in I_r$ and $m \in M_{ri}$. The second term is the fixed cost for all ships deployed. It should be noted that the ships not deployed on these routes have alternative values. For instance, they can be chartered out. The fixed cost of these ships thus will not be included in our objective function. The third term is the total dockage refund obtained by participating in the VSRIPs. Constraints (2) state that the total sailing time of all stretches on a route is equal to the rotation time of the route minus its total port time. Constraint (3) limits the number of ships deployed on routes. Recall that the VSRZ is always within the ECA for ES ports. The sailing distances within and outside ECAs on a leg can be determined by Constraints (4) and (5). Constraints (6) ensure that only one path can be chosen for a leg. Constraints (7) and (8) state that the sailing distance within VSRZ is decided by the choice of VSRZ since the radius of each VSRZ is fixed, and only one VSRZ can be chosen at a port by Constraints (9). Constraints (10) guarantee the sailing speed on each stretch does not exceed the speed limit. All variables in the model are defined in Constraints (11)–(15).

## 3. A dynamic programming based method

The joint liner ship path, speed, and deployment problem of all routes are connected by Constraint (3) that entails the limited ship fleet size deployed on these routes. Therefore, given the number of ships deployed on a route $r$, we can optimize the sailing path, the sailing speeds, and the compliance of VSRIPs on this route independently. Taking advantage of this property, a tailored algorithm based on analytical solutions and dynamic programming is developed.

### *3.1. One route optimization without considering the limitation of fleet size*

In this section, we do not consider the limited number of ships, i.e., remove Constraint (3), and we will analyze how to optimize the number of ships deployed, the sailing path and speeds, and the compliance of VSRIPs for a route $r$ including ECA ports, VSRZ ports, ES ports, and non-ES ports. Given the number of ships deployed, we will optimize sailing speed and construct the super path set for a route with only ECA ports and non-ES ports in Section 3.1.1. Based on the results above, a route with all types of ports will be analyzed in Section 3.1.2, and for a given number of ship deployed, the optimal solution of the route on the sailing path and speeds and the compliance of VSRIPs can be obtained, which is treated as input for Section 3.1.3. An algorithm is developed in Section 3.1.3 for deriving the optimal number of ships deployed on route $r$ with all types of ports. A route not covering all types of ports is a special case of the route with all types of ports, which can also be optimized by the proposed method in this section. For example, for a route with only VSRZ ports and non-ES ports, ships will always sail along the shortest path, and the optimal decisions on the number of ships deployed, the sailing speeds, and the program compliance can be made by Sections 3.1.2 and 3.1.3.

#### *3.1.1. A route covering only ECA and non-ES ports with given number of ships deployed*

For a route $r$ covering only ECAs without VSRZs, ships should sail at one speed within ECAs and at another speed outside ECAs. Therefore, route $r$ can be regarded as a "super leg" with two parts: within ECAs and outside ECAs. Given the number of deployed ships $\tilde{q}_r$, we need to determine the choice of sailing path and minimize the cost of the route, i.e., the sum of fuel cost and carbon tax. Define $x_r^E = \sum_{i \in I_r} \sum_{m \in M_{ri}^E} x_{rim}$, $x_r^N = \sum_{i \in I_r} \sum_{m \in M_{ri}^N} x_{rim}$, $t_r^E = \sum_{i \in I_r} \sum_{m \in M_{ri}^E} t_{rim}$ and $t_r^N = \sum_{i \in I_r} \sum_{m \in M_{ri}^N} t_{rim}$. The sailing time outside ECAs $t_r^N$ is equal to $T \cdot \tilde{q}_r - T_r - t_r^E$. The cost function $f(x_r^E, x_r^N, t_r^E, t_r^N, \tilde{q}_r)$ for route $r$ is:

$$f(x_r^E, x_r^N, t_r^E, t_r^N, \tilde{q}_r) = (\alpha^E + c^{CO_2})x_r^E \cdot a\left(\frac{x_r^E}{t_r^E}\right)^b + (\alpha^N + c^{CO_2})x_r^N \cdot a\left(\frac{x_r^N}{T \cdot \tilde{q}_r - T_r - t_r^E}\right)^b. \tag{16}$$

The function $f(x_r^E, x_r^N, t_r^E, t_r^N, \tilde{q}_r)$ is convex in $t_r^E$, whose optimal solution $t_r^{E*}$ related to variables $x_r^E$ and $x_r^N$ can be obtained by mathematical analysis.

$$t_r^{E*} = \begin{cases} T \cdot \tilde{q}_r - T_r - \frac{x_r^N}{V^{\max}}, & q_r^{\min} \leq \tilde{q}_r < \hat{q}_r \\ \frac{\beta x_r^E}{\beta x_r^E + x_r^N}(T \cdot \tilde{q}_r - T_r), & \tilde{q}_r \geq \hat{q}_r, \end{cases} \tag{17}$$

where $\beta = [(\alpha^E + c^{CO_2})/(\alpha^N + c^{CO_2})]^{1/(b+1)}$, $q_r^{\min} = \lceil [(x_r^E + x_r^N)/V^{\max} + T_r]/T \rceil$ and $\hat{q}_r = \lceil [(\beta x_r^E + x_r^N)/V^{\max} + T_r]/T \rceil$ ($\lceil \theta \rceil$ is the smallest integer greater than or equal to $\theta$). Plugging Eq. (17) into Eq. (16), the minimum cost of route $r$ on $x_r^E$ and $x_r^N$ is

$$f(x_r^E, x_r^N, t_r^{E*}, t_r^{N*}, \tilde{q}_r) = \begin{cases} (\alpha^E + c^{CO_2}) \cdot (x_r^E)^{b+1} \cdot a(T \cdot \tilde{q}_r - T_r - \frac{x_r^N}{V^{\max}})^{-b} & \\ +(\alpha^N + c^{CO_2}) \cdot x_r^N \cdot a(V^{\max})^b, & q_r^{\min} \leq \tilde{q}_r < \hat{q}_r \\ (\alpha^N + c^{CO_2}) \cdot (\beta x_r^E + x_r^N)^{b+1} \cdot a(T \cdot \tilde{q}_r - T_r)^{-b}, & \tilde{q}_r \geq \hat{q}_r. \end{cases} \tag{18}$$

We can see from Eq. (18) that the minimum cost of the route as well as the values of $q_r^{\min}$ and $\hat{q}_r$ is dependent on the choice of sailing path. When $q_r^{\min} \leq \tilde{q}_r < \hat{q}_r$, the optimal sailing speeds within and outside ECAs are $x_r^E/(T \cdot \tilde{q}_r - T_r - x_r^N/V^{\max})$ and $V^{\max}$, respectively; when $\tilde{q}_r \geq \hat{q}_r$, their optimal speeds are $[x_r^E + (1/\beta)x_r^N]/(T \cdot \tilde{q}_r - T_r)$ and $(\beta x_r^E + x_r^N)/(T \cdot \tilde{q}_r - T_r)$, respectively. We find that the optimal speed outside ECAs is $\beta$ times that within ECAs when $\tilde{q}_r \geq \hat{q}_r$, while the sailing speeds within and outside ECAs are not proportional when $q_r^{\min} \leq \tilde{q}_r < \hat{q}_r$ due to the maximum physical speed of ships. Therefore, the minimum cost functions of route $r$ are different when $q_r^{\min} \leq \tilde{q}_r < \hat{q}_r$ and when $\tilde{q}_r \geq \hat{q}_r$. To construct the super path for route $r$, we will discuss the choice of paths for the legs on the route first. (i) For a leg with two non-ES ports, the shortest path will be chosen. (ii) For a leg with an ECA port and a non-ES port, infinite detour points can be found on the ECA boundary, and a path consists of a sailing from a port to a detour point and from the detour point to the next port (see Fig. 4). As a result, there exist infinite sailing paths for each leg. We will discretize the ECA boundary with a unit distance, such as 1 nm. To reduce the number of feasible sailing paths, a path with a longer distance within ECA and a longer total distance than another path should be removed. As shown in Fig. 4, we will only maintain the paths with detour points between C and D on the ECA boundary because it is evident that these paths are superior than the paths with detour points E and F. (iii) For

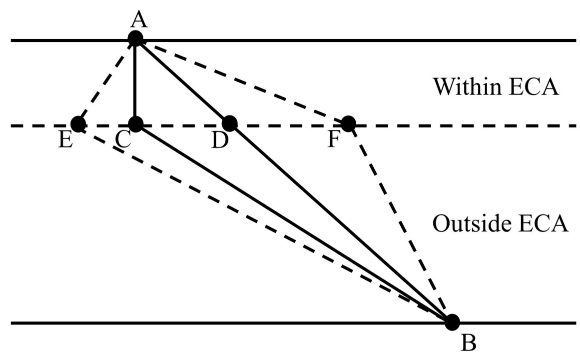


Figure 4: Detour points illustration

a leg with two ECA ports, including two ECA ports in the same ECA and in two different ECAs, its paths can be reduced by the similar method. Note that if a leg has two ECA ports in the same ECA, the shortest path totally covered by the ECA will be maintained. Then the algorithm for searching a set of super paths for route $r$ is organized as follows.

**Proposition 1.** *The choice of super paths that can be included in set $L_r$ obeys the following rules: for every two super paths $l_1$ and $l_2$ ($d^E_{rl_1} < d^E_{rl_2}$), (i) if $d^E_{rl_1} + d^N_{rl_1} \leq d^E_{rl_2} + d^N_{rl_2}$, super path $l_2$ should be removed; (ii) if $d^E_{rl_1} + d^N_{rl_1} > d^E_{rl_2} + d^N_{rl_2}$ and $\beta d^E_{rl_1} + d^N_{rl_1} \geq \beta d^E_{rl_2} + d^N_{rl_2}$, super path $l_1$ should be removed; (iii) if $d^E_{rl_1} + d^N_{rl_1} > d^E_{rl_2} + d^N_{rl_2}$ and $\beta d^E_{rl_1} + d^N_{rl_1} < \beta d^E_{rl_2} + d^N_{rl_2}$, both super paths should be maintained.*

*Proof.* See Appendix A □

*3.1.2. A route covering all types of ports with given number of ships deployed*

A route $r$ with ECA ports, VSRZ ports, ES ports, and non-ES ports is studied in this section. The aim of this section is to optimize the path and speeds of the route, as well as the compliance of VSRZs $y_r$ ($y_r$ is all vectors of $y_{rpj}, p \in P^S_r \cup P^{ES}_r, j \in J_{rp}$). We will first analyze the cost function including fuel cost and carbon tax minus dockage refund for route $r$ with $\tilde{q}_r$ ships. Redefine $x^E_r = \sum_{i\in I_r} \sum_{m\in M^E_{ri} \cup M^{ES}_{ri}} x_{rim}$ and $x^N_r = \sum_{i\in I_r} \sum_{m\in M^S_{ri} \cup M^N_{ri}} x_{rim}$. Note that one chosen VSRZ at a VSRZ or ES port is

**Algorithm 1** Derive a set of super paths for route $r$

**Step 0.** Initialize the unit distance for path discretization, denoted by $\Delta$ (e.g., 1 nm).

**Step 1.** For each leg $i \in I_r$, round up the sailing distances within and outside ECAs for each path $k \in K_{ri}$: $d^E_{rik} \leftarrow \lceil d^E_{rik}/\Delta \rceil \Delta$ and $d^N_{rik} \leftarrow \lceil d^N_{rik}/\Delta \rceil \Delta$.

**Step 2.** Calculate the maximum and minimum sailing distances within ECAs of super paths for route $r$, denoted by $d^{E\max}_r$ and $d^{E\min}_r$, respectively. $d^{E\max}_r = \sum_{i=1}^{I_r} \max_{k\in K_{ri}} d^E_{rik}$ and $d^{E\min}_r = \sum_{i=1}^{I_r} \min_{k\in K_{ri}} d^E_{rik}$.

**Step 3.** For each $k = 0, 1, ..., (d^{E\max}_r - d^{E\min}_r)/\Delta$, use dynamic programming to find the super path with the shortest sailing distance outside ECAs such that its sailing distance within ECAs is not greater than $d^{E\min}_r + k \cdot \Delta$.

**Step 4.** Some super paths identified in **Step 3** may be identical and only one of them needs to be maintained. Further, some super paths can be removed by Proposition 1, and the remaining super paths comprise $L_r$. The number of super paths in $L_r$ does not exceed $(d^{E\max}_r - d^{E\min}_r)/\Delta + 1$.

---

related to two legs and the speed limit of the VSRZ should be obeyed when ships approach to and depart from the port. Therefore, we define $D^{ES}_r = \sum_{p\in P^{ES}_r} \sum_{j\in J_{rp}} 2d_{rpj}y_{rpj}$, $D^S_r = \sum_{p\in P^S_r} \sum_{j\in J_{rp}} 2d_{rpj}y_{rpj}$, and $C^{ref}_r = \sum_{p\in P^S_r \cup P^{ES}_r} \sum_{j\in J_{rp}} c^{ref}_{rpj}y_{rpj}$. The method for constructing the set of super paths and some optimal results on the sailing path and the sailing speeds within and outside ECAs in Section 3.1.1 are also applicable for the route with all types of ports. If the optimal sailing speed within ECAs is less than $V^S$, the speed within the chosen VSRZs at ES ports is equal to that within ECAs, and otherwise the speed within these VSRZs is $V^S$. Similarly, the sailing speeds within the chosen VSRZs at VSRZ ports can be determined. Therefore, for a given super path and a given compliance of VSRZs, we can design the optimal sailing speed for each stretch of route $r$. We denote by $t^{E*}_r$, $t^{S*}_r$, $t^{ES*}_r$, and $t^{N*}_r$ the optimal solutions of $t_{rim}$ for all $m \in M^E_{ri}$, $m \in M^S_{ri}$, $m \in M^{ES}_{ri}$, and $m \in M^N_{ri}$ and $i \in I_r$, respectively, which are related to the variables $x^E_r$, $x^N_r$ and $y_r$. We assume $\beta V^S < V^{\max}$ based on real data. There are four cases on the cost function $g(x^E_r, x^N_r, t^{E*}_r, t^{S*}_r, t^{ES*}_r, t^{N*}_r, \tilde{q}_r, y_r)$ of route $r$ due to the maximum physical speed of ships and the speed limit within VSRZs, which will be analyzed specifically by first defining $q^{\min}_r =$

$\lceil[(x_r^E - D_r^{ES})V^S + (x_r^N - D_r^S)V^S + T_r V^{\max} V^S + (D_r^{ES} + D_r^S)V^{\max}]/(T \cdot V^{\max} V^S)\rceil$, $\hat{q}_r^E = \lceil[\beta(x_r^E - D_r^{ES})V^S + (x_r^N - D_r^S)V^S + T_r V^{\max} V^S + (D_r^{ES} + D_r^S)V^{\max}]/(T \cdot V^{\max} V^S)\rceil$, $\hat{q}_r^{ES} = \lceil[\beta x_r^E + (x_r^N - D_r^S) + \beta T_r V^S + \beta D_r^S]/(\beta T \cdot V^S)\rceil$, and $\hat{q}_r^S = \lceil(\beta x_r^E + x_r^N + T_r V^S)/(T \cdot V^S)\rceil$.

(i) When $q_r^{\min} \leq \tilde{q}_r < \hat{q}_r^E$, the sailing speed outside ECAs is restricted by the maximum physical speed of ships $V^{\max}$, and thus ships sail at higher than $V^{\max}/\beta$ within ECAs and at $V^{\max}$ outside. The sailing speeds within chosen VSRZs at VSRZ and ES ports are equal to the speed limit in the VSRIPs $V^S$. The cost function $g(x_r^E, x_r^N, t_r^{E*}, t_r^{S*}, t_r^{ES*}, t_r^{N*}, \tilde{q}_r, y_r)$ can be written as

$$\begin{aligned} & g(x_r^E, x_r^N, t_r^{E*}, t_r^{S*}, t_r^{ES*}, t_r^{N*}, \tilde{q}_r, y_r) \\ &= (\alpha^E + c^{CO_2})[(x_r^E - D_r^{ES})^{b+1} a(T \cdot \tilde{q}_r - T_r - \frac{x_r^N - D_r^S}{V^{\max}} - \frac{D_r^{ES} + D_r^S}{V^S})^{-b} + D_r^{ES} \cdot a(V^S)^b] \\ & \quad + (\alpha^N + c^{CO_2})[(x_r^N - D_r^S) \cdot a(V^{\max})^b + D_r^S \cdot a(V^S)^b] - C_r^{ref}. \end{aligned} \tag{19}$$

(ii) When $\hat{q}_r^E \leq \tilde{q}_r < \hat{q}_r^{ES}$, the ratio of the sailing speed within ECAs to that outside is $1/\beta$, and both sailing speeds are higher than $V^S$, while the sailing speed within each chosen VSRZ is equal to $V^S$. Hence, we have

$$\begin{aligned} & g(x_r^E, x_r^N, t_r^{E*}, t_r^{S*}, t_r^{ES*}, t_r^{N*}, \tilde{q}_r, y_r) \\ &= (\alpha^N + c^{CO_2})[\beta(x_r^E - D_r^{ES}) + (x_r^N - D_r^S)]^{b+1} \cdot a(T \cdot \tilde{q}_r - T_r - \frac{D_r^{ES} + D_r^S}{V^S})^{-b} \\ & \quad + [(\alpha^E + c^{CO_2})D_r^{ES} + (\alpha^N + c^{CO_2})D_r^S] \cdot a(V^S)^b - C_r^{ref}. \end{aligned} \tag{20}$$

(iii) When $\hat{q}_r^{ES} \leq \tilde{q}_r < \hat{q}_r^S$, the sailing speed within ECAs will be no higher than $V^S$, and ships therefore will participate in all VSRIPs at ES ports in the optimal solution. The sailing speed outside ECAs will be higher than $V^S$, and the sailing speed within chosen VSRZs at VSRZ ports should be $V^S$. Then the cost function is

$$\begin{aligned} & g(x_r^E, x_r^N, t_r^{E*}, t_r^{S*}, t_r^{ES*}, t_r^{N*}, \tilde{q}_r, y_r) \\ &= (\alpha^N + c^{CO_2})[\beta x_r^E + (x_r^N - D_r^S)]^{b+1} \cdot a(T \cdot \tilde{q}_r - T_r - \frac{D_r^S}{V^S})^{-b} + (\alpha^N + c^{CO_2})D_r^S \cdot a(V^S)^b - C_r^{ref}. \end{aligned} \tag{21}$$

(iv) When $\tilde{q}_r \geq \hat{q}_r^S$, the sailing speeds within and outside ECAs are no higher than $V^S$ so that in the optimal solution all VSRIPs at VSRZ and ES ports will be obeyed. We therefore have the following cost function.

$$g(x_r^E, x_r^N, t_r^{E*}, t_r^{S*}, t_r^{ES*}, t_r^{N*}, \tilde{q}_r, y_r) = (\alpha^N + c^{CO_2})(\beta x_r^E + x_r^N)^{b+1} \cdot a(T \cdot \tilde{q}_r - T_r)^{-b} - C_r^{ref}. \quad (22)$$

From the analysis above, we observe an important finding as follows.

**Proposition 2.** *Given super path $l$ for route $r$, all VSRIPs at VSRZ and ES ports should be complied with so as to minimize the cost including fuel cost and carbon tax minus dockage refund when $\tilde{q}_r \geq \hat{q}_{rl}^S$ ($\hat{q}_{rl}^S = \lceil (\beta d_{rl}^E + d_{rl}^N + T_r V^S)/(T \cdot V^S) \rceil$).*

**Proposition 3.** *Given super path $l$ for route $r$, the compliance of VSRZs follows the rules below: (i) if some VSRZs of ES ports (VSRZ ports) on route $r$ have the same radius, the speed limit in the VSRZ with the higher refund will be obeyed first; (ii) if some VSRZ groups have the same VSRZ and ES distances, the speed limit in the VSRZ group with the higher total dockage refund will be obeyed first.*

*Proof.* See Appendix B. □

Define $\hat{q}_r^{E,\max} = \left\lceil [\beta(d_{rl^{\max}}^E - D_r^{ES,\max})V^S + (d_{rl^{\max}}^N - D_r^{S,\max})V^S + T_r V^{\max} V^S + (D_r^{ES,\max} + D_r^{S,\max})V^{\max}]/(T \cdot V^{\max} V^S) \right\rceil$, where $D_r^{ES,\max} = \sum_{p \in P_r^{ES}} 2d_{rp|J_{rp}|}$, $D_r^{S,\max} = \sum_{p \in P_r^S} 2d_{rp|J_{rp}|}$, and $l^{\max}$ is the super path with the maximum $\beta d_{rl}^E + d_{rl}^N$ among all super paths $l \in L_r$. We have the following proposition:

**Proposition 4.** *When $\tilde{q}_r \geq \hat{q}_r^{E,\max}$, the super path with the minimum $\beta d_{rl}^E + d_{rl}^N$ for all $l \in L_r$ is the optimal one for route $r$ covering all types of ports under each compliance of VSRZs at VSRZ and ES ports*

*Proof.* See Appendix C. □

With a given number of deployed ships, the sailing path, the sailing speeds, and the compliance of VSRZs on the route can be derived by Algorithm 2.

Comparing the cases with and without the carbon tax, we have one more proposition as below:

**Proposition 5.** *The total distance of the optimal super path when the carbon tax is considered will be shorter than or equal to that when there is no carbon tax.*

*Proof.* See Appendix D. □

**Algorithm 2** One route optimization with given number of deployed ships $\tilde{q}_r$

Input $\tilde{q}_r$, all VSRIPs at VSRZ and ES ports, and all super paths obtained by Algorithm 1.
Output the optimal sailing path and speeds and the optimal compliance of all VSRIPs on route $r$.

```
if q̃_r ≥ q̂_r^{E,max} then
    Remove the super paths in the set L_r except the super path with the minimum
    βd_{rl}^E + d_{rl}^N among all super paths l ∈ L_r.
end if
for each super path l ∈ L_r do
    Calculate q̂_{rl}^S.
    if q̃_r ≥ q̂_{rl}^S then
        All VSRIPs at VSRZ and ES ports will be complied with, and the optimal sailing
        speeds will be calculated by Eq. (22).
    else
        Enumerate the VSRZ and ES distances of VSRZ groups.
        for each VSRZ distance do
            for each ES distance do
                Referring to Proposition 3, construct the optimal VSRZ groups that has
                higher total dockage refund by comparing with other VSRZ groups with
                the same VSRZ and ES distances.
            end for
        end for
        Identify the optimal sailing speeds and compliance of VSRZs for route r with the
        minimum cost by Eqs. (19), (20), and (21).
    end if
end for
Compare the minimum cost of each super path and obtain the optimal super path.
```

Fagerholt et al. (2015) and Fagerholt and Psaraftis (2015) have pointed out that ECAs will lead to the detour of ships, in which case the total shipping emissions will increase. Our finding in Proposition 5 indicates that the detour issue can be mitigated by introducing a carbon tax into the shipping industry.

#### *3.1.3. The optimal number of ships deployed on a route with all types of ports*

As discussed in Section 3.1.2, the optimal sailing path and speeds on a route $r$ can be determined for a given number of ships deployed. On top of this, we will explore how to optimize the number of ships deployed on the route considering its total cost (fuel cost, carbon tax, and fixed cost, minus dockage refund) in this section. The total cost function $h(x_r^E, x_r^N, t_r^{E*}, t_r^{S*}, t_r^{ES*}, t_r^{N*}, q_r, y_r)$ is

$$h(x_r^E, x_r^N, t_r^{E*}, t_r^{S*}, t_r^{ES*}, t_r^{N*}, q_r, y_r) = g(x_r^E, x_r^N, t_r^{E*}, t_r^{S*}, t_r^{ES*}, t_r^{N*}, q_r, y_r) + c^{fix} q_r. \quad (23)$$

In this function, $x_r^E$, $x_r^N$, $y_r$, and $q_r$ are variables, and $t_r^{E*}, t_r^{S*}, t_r^{ES*}, t_r^{N*}$ are the optimal solutions related to these variables. Define $q_r^{\text{MIN}} = \lceil [(d^E_{rl^{\min}} + d^N_{rl^{\min}})/V^{\max} + T_r]/T \rceil$ ($l^{\min}$ is the super path with the shortest total sailing distance) and $\hat{q}_r^{S,\max} = \lceil (\beta d^E_{rl^{\max}} + d^N_{rl^{\max}} + T_r V^S)/(T \cdot V^S) \rceil$. The property of function (23) is organized as follows.

**Proposition 6.** *Assume $q_r$ can take fractional quantities. When $q_r^{\text{MIN}} \leq q_r < \hat{q}_r^{S,\max}$, the total cost function (23) is non-convex in $q_r$; when $q_r \geq \hat{q}_r^{S,\max}$, the total cost function is convex in $q_r$.*

*Proof.* See Appendix E. □

The optimal number of ships deployed on route $r$ can be obtained by Algorithm 3.

### *3.2. Optimization for all routes (i.e., solving model [$\mathbb{P}$])*

Since the total number of ships in the shipping company is limited, it is likely that the total optimal number of ships deployed for all routes that is calculated by Section 3.1.3 cannot be satisfied. To address the fleet deployment problem on all routes, we will reconsider constraint (3) regarding the limited number of ships in the company in this section. Define $U(r, Q_r)$ as the minimum total cost of routes $1, ..., r$ for all $r = 1, ..., |R|$ and state $Q_r = \sum_{r'=1}^{r} q_{r'}^{\text{MIN}}, ..., \min\{\sum_{r'=1}^{r} q_{r'}^{*}, Q - \sum_{r'=r+1}^{|R|} q_{r'}^{\text{MIN}}\}$, where $Q_r$ is the number of ships deployed on routes $1, ..., r$. Based on the results of Algorithm 3, a

**Algorithm 3** Derive the optimal number of ships deployed on route $r$

Set $q_r \leftarrow q_r^{\mathrm{MIN}}$. Optimize the sailing path and speeds and the compliance of VSRZs by Algorithm 2, and calculate the minimum total cost $C_r^{\min}(q_r)$.

  **do**

    Set $q_r \leftarrow q_r + 1$. Optimize the sailing path and speeds and the compliance of VSRZs by Algorithm 2, and calculate the minimum total cost $C_r^{\min}(q_r)$.

  **while** $q_r \leq \hat{q}_r^{S,\max}$ or $C_r^{\min}(q_r) < C_r^{\min}(q_r - 1)$ and $q_r + 1 \leq Q - \sum_{r' \in R \setminus \{r\}} q_{r'}^{\mathrm{MIN}}$

Set $q_r^{\max} \leftarrow q_r$. Identify the optimal number of ships deployed $q_r^*$ by comparing $C_r^{\min}(q_r)$ for all $q_r^{\mathrm{MIN}} \leq q_r \leq q_r^{\max}$.

dynamic programming based algorithm for optimizing the fleet deployment of all routes and the sailing path, the sailing speeds, and the compliance of VSRIPs of each route is developed.

**Algorithm 4** Optimization of all routes based on dynamic programming

Calculate $q_r^*$ and obtain $C_r^{\min}(q_r)$ for all $q_r = q_r^{\mathrm{MIN}}, ..., q_r^*$ and $r \in R$ by Algorithm 3.

  **if** $\sum_{r \in R} q_r^* \leq Q$ **then**

    Deploy $q_r^*$ ships for route $r \in R$.

  **else**

    Set $r \leftarrow 1$ and $U(r, Q_r) = C_r^{\min}(Q_r)$ for all $Q_r = q_r^{\mathrm{MIN}}, ..., \min\{q_r^*, Q - \sum_{r'=r+1}^{|R|} q_{r'}^{\mathrm{MIN}}\}$.

    **do**

      Set $r \leftarrow r + 1$ and $Q_r \leftarrow \sum_{r'=1}^{r} q_{r'}^{\mathrm{MIN}}$.

      **do**

        Set $U(r, Q_r) = \min_{q_r = q_r^{\mathrm{MIN}}, ..., \min\{q_r^*, Q - \sum_{r' \in R \setminus \{r\}} q_{r'}^{\mathrm{MIN}}\}} [C_r^{\min}(q_r) + U(r - 1, Q_r - q_r)]$, and set $Q_r \leftarrow Q_r + 1$.

      **while** $Q_r \leq \min\{\sum_{r'=1}^{r} q_{r'}^*, Q - \sum_{r'=r+1}^{|R|} q_{r'}^{\mathrm{MIN}}\}$

    **while** $r < |R|$

    Calculate the minimum total cost of all routes $U^{\min}$ by $U^{\min} = \min_{Q_{|R|} = \sum_{r \in R} q_r^{\mathrm{MIN}}, ..., Q} U(|R|, Q_{|R|})$.

  **end if**

**Proposition 7.** *Given the values of the minimum total cost $C_r^{\min}(q_r)$ for all $r \in R$ and $q_r = q_r^{\mathrm{MIN}}, ..., \min\{q_r^*, Q - \sum_{r' \in R \setminus \{r\}} q_{r'}^{\mathrm{MIN}}\}$, Algorithm 4 can optimize the fleet deployment problem in time bounded by $O\left(|R| \cdot Q^2\right)$ when $\sum_{r \in R} q_r^* > Q$.*

*Proof.* See Appendix F. $\square$

## 4. Numerical experiments

We conduct extensive numerical experiments in this section in order to examine the effectiveness of the proposed model and the efficiency of the tailored algorithm based on dynamic programming. These experiments are performed on a personal computer with a 2.5 GHz Intel Core i7 and 8 GB RAM, and the tailored algorithm is implemented in the programming language C# (VS2012).

The experimental data are generated based on the practical condition and the existing literature. We collect the information of real ports, and some ports are selected randomly to construct the routes in our experiments. The time spent at each port of call on a route follows a uniform distribution [12, 60] hours (Qi and Song, 2012). We investigate a liner shipping company with a large number of 10,000-TEU ships whose maximum speed is 25 knots. The fixed cost per ship is set to be 387,000 USD/week (Sheng et al., 2017; Shin et al., 2019). Referring to the global average fuel prices from January to March in 2020, the price of 0.5% low-sulfur fuel and 0.1% low-sulfur fuel are 500 USD/ton and 600 USD/ton, respectively (Ship and Bunker, 2020). The conversion factors $a$ and $b$ between fuel consumption per unit distance and sailing speed are $4.7 \times 10^{-4}$ and 2.118 (Wang and Meng, 2012). The total number of ships in each experimental instance is generated taking into account the total sailing distance of all routes and the total time spent at all ports of call.

We set up the parameters of the three emission reduction measures as follows. (i) We study the four international ECAs in our experiment, and their boundaries are discretized by the unit distance of 10 nm. The discretization points can be used to derive the sailing paths for the legs covering ECAs. (ii) The carbon tax is set to 76 USD per ton fuel according to the average $CO_2$ price in the European carbon trading market during the first three months of 2020 (ICE, 2020). (iii) In addition to ports of LA, Long Beach, San Diego, and New York and New Jersey and several ports in South Korea, which have already adopted VSRIPs, we also design some other ports with VSRIPs randomly since the adoption of VSRIPs is under discussion at some ports. In our instances, each VSRIP has one or two VSRZs, whose radii can be 20 or 40 nm and speed limit is 12 knots. The dockage refunds per ship visit for 20 nm and 40 nm VSRZs are generated randomly between 1,000 and 2,000 USD and between 2,000 and 3,000 USD, respectively (Zhuge et al., 2020).

### 4.1. Performance of the proposed model and algorithm

To validate the effectiveness of the proposed model, we compare the solution of model [$\mathbb{P}$] (denoted by $\text{obj}_0$) with the solution without considering any measure ($\text{obj}_1$), the solution without considering ECAs ($\text{obj}_2$), the solution without considering carbon tax ($\text{obj}_3$), and the solution without considering VSRIPs ($\text{obj}_4$), respectively. When the shipping company makes a decision without considering any emission reduction measure, the ships will sail along the shortest super path at the average speed on each route, and the fleet deployment problem can be addressed easily. Under three emission reduction measures, we can obtain $\text{obj}_1$ by plugging these decisions into the objective function of model [$\mathbb{P}$]. When the ECAs are not considered, i.e., only carbon tax and VSRIPs are included, the shortest super path will be chosen for each route, and we can optimize fleet deployment, sailing speeds, and compliance of VSRIPs by combining Algorithms 2, 3, and 4. These decisions will be put into the objective function of model [$\mathbb{P}$] for calculating $\text{obj}_2$ under all of the three measures. When we ignore the carbon tax in decision-making process, all algorithms developed in our study will be called to obtain the optimal fleet deployment, sailing path and speed, and program compliance, which will be substituted into objective function (1) for generating $\text{obj}_3$. When we do not take into account VSRIPs, the optimal decisions on fleet deployment, and sailing path and speed can be obtained by the proposed algorithms with some simplifications. Under all emission reduction measures, ships can obtain the dockage refund if the designed sailing speed is lower than or equal to the speed limit in a VSRZ, and similarly, these decisions will be used for obtaining $\text{obj}_4$.

Three experimental groups with 10, 20, and 30 routes are conducted, and each group consists of five instances. The computational results on the comparison between $\text{obj}_0$ and $\text{obj}_1$, $\text{obj}_2$, $\text{obj}_3$, or $\text{obj}_4$ are shown in Table 1. The values of "$\text{Gap}_1$" show that considering three emission reduction measures can save more than 0.5% of the total cost. Note that the 0.5% cost saving is significant since the operating cost per week in some well-known international shipping lines can be as high as 100 million dollars. The gap between considering three measures and not considering ECAs (i.e., $\text{Gap}_2$) is over 0.4% for each instance, which demonstrates the importance of introducing ECAs into shipping network design. The values of $\text{Gap}_3$ are between 0.0020% and 0.1882% for the fifteen instances, which is because the effect of carbon tax on path choice varies for each instance. That is, if the carbon tax impacts the choice of super path significantly in an instance, then the gap between considering three measures and not considering carbon tax is large; otherwise, the gap is small. The values of $\text{Gap}_4$ are also unstable with a range from 0.0012% to 0.0925%.

It makes sense since the number of VSRZ ports and ES ports included in each instance is different and the compliance of VSRIPs is related to the details of each instance.

We have identified that sulfur emission regulations, carbon tax, and VSRIPs have different impacts on sailing path and speed. The results in Table 1 have reported that the solutions obtained without simultaneous consideration of the three measures are sub-optimal. In contrast, the proposed model can provide better suggestions on how to design sailing path, sailing speed, and fleet deployment for different liner service routes under the three emission reduction measures. Our analysis results can also help shipping companies make a wiser decision on the compliance of VSRIPs for reducing the cost. Consider an example of an Asia-US Southwest Coast service route in COSCO shipping lines with the fixed sequence of ports of call visited as follows: Qingdao, Shanghai, Ningbo, LA, Oakland, Tokyo, and Qingdao. We can give the operational guideline on the numbers of ships deployed on the route, the compliance of VSRIPs at LA, the sailing path of each leg, and the sailing speeds within ECAs near LA and Oakland, within chosen VSRZs, and outside the two areas.

We explore the efficiency of the tailored algorithm based on dynamic programming by observing the computation time of experimental instances. Each instance, including the instance with 30 routes, can be solved within 20 seconds, which indicates that the tailored algorithm is highly efficient for solving the proposed model. We also solve the proposed problem by the CPLEX solver based on the results of Algorithms 1, 2, and 3 to facilitate a direct comparison with the solution from the dynamic programming based method. We find that the method proposed in our study performs slightly better.

Table 1: Effectiveness of the proposed model and efficiency of the tailored algorithm

| Instances | model [$\mathbb{P}$] | | Not consider any measure | | Not consider ECAs | | Not consider carbon tax | | Not consider VSRIPs | |
|---|---|---|---|---|---|---|---|---|---|---|
| | $obj_0$ | CPU time (s) | $obj_1$ | $Gap_1$ | $obj_2$ | $Gap_2$ | $obj_3$ | $Gap_3$ | $obj_4$ | $Gap_4$ |
| 10-1 | 29,724,963 | 5 | 29,886,460 | 0.54% | 29,885,389 | 0.54% | 29,725,708 | 0.0025% | 29,726,033 | 0.0036% |
| 10-2 | 30,623,662 | 4 | 30,812,244 | 0.62% | 30,811,931 | 0.61% | 30,624,554 | 0.0029% | 30,624,029 | 0.0012% |
| 10-3 | 31,656,305 | 6 | 31,817,464 | 0.51% | 31,810,656 | 0.49% | 31,657,344 | 0.0033% | 31,663,722 | 0.0234% |
| 10-4 | 29,640,525 | 4 | 29,803,720 | 0.55% | 29,791,591 | 0.51% | 29,688,592 | 0.1622% | 29,657,813 | 0.0583% |
| 10-5 | 28,233,563 | 5 | 28,379,443 | 0.52% | 28,357,551 | 0.44% | 28,252,817 | 0.0682% | 28,259,678 | 0.0925% |
| 20-1 | 60,529,811 | 10 | 60,846,627 | 0.52% | 60,842,829 | 0.52% | 60,531,152 | 0.0022% | 60,533,684 | 0.0064% |
| 20-2 | 56,949,242 | 9 | 57,265,824 | 0.56% | 57,202,376 | 0.44% | 57,052,366 | 0.1811% | 56,989,053 | 0.0699% |
| 20-3 | 57,275,443 | 11 | 57,577,879 | 0.53% | 57,508,343 | 0.41% | 57,369,943 | 0.1650% | 57,309,809 | 0.0600% |
| 20-4 | 58,023,066 | 10 | 58,326,189 | 0.52% | 58,315,770 | 0.50% | 58,024,203 | 0.0020% | 58,033,775 | 0.0185% |
| 20-5 | 59,708,036 | 10 | 60,022,265 | 0.53% | 60,016,890 | 0.52% | 59,709,762 | 0.0029% | 59,713,848 | 0.0097% |
| 30-1 | 85,286,845 | 15 | 85,738,273 | 0.53% | 85,641,040 | 0.42% | 85,402,260 | 0.1353% | 85,363,536 | 0.0899% |
| 30-2 | 96,958,871 | 16 | 97,468,194 | 0.53% | 97,463,446 | 0.52% | 96,961,335 | 0.0025% | 96,963,863 | 0.0051% |
| 30-3 | 94,825,817 | 18 | 95,373,720 | 0.58% | 95,372,343 | 0.58% | 94,828,360 | 0.0027% | 94,827,622 | 0.0019% |
| 30-4 | 92,100,695 | 17 | 92,607,555 | 0.55% | 92,593,240 | 0.53% | 92,103,088 | 0.0026% | 92,115,522 | 0.0161% |
| 30-5 | 87,114,122 | 15 | 87,556,189 | 0.51% | 87,525,181 | 0.47% | 87,278,078 | 0.1882% | 87,162,475 | 0.0555% |

Notes:
(i) Instance "10-1" is the first instance in the group of 10 routes.
(ii) $Gap_1 = (obj_1 - obj_0)/obj_0$, $Gap_2 = (obj_2 - obj_0)/obj_0$, $Gap_3 = (obj_3 - obj_0)/obj_0$, and $Gap_4 = (obj_4 - obj_0)/obj_0$.

### 4.2. Sensitivity analysis

The bunker price may have a significant fluctuation due to the implementation of the 0.5% global sulfur limit and some important events (e.g., the outbreak of COVID-19), and the $CO_2$ price also varies every year (ICE, 2020). In this section, we will investigate the impacts of the fuel prices (i.e., MGO price and VLSFO price) and carbon tax on the effectiveness of the model considering sulfur limit regulations, carbon tax and VSRIPs by analyzing the five instances with 10 routes in Table 1.

We examine the sensitivity of fuel price by two groups of experiments as follows: changing only the MGO price in group 1, i.e., designing six MGO prices (520, 560, 600, 640, 680, and 720 USD/ton); changing only the VLSFO price in group 2, i.e., designing six VLSFO prices (260, 320, 380, 440, 500, and 560 USD/ton). The results of group 1 (see Fig. 5) and group 2 (see Fig. 6) indicate that fuel price has a great impact on the gap between the total cost considering three emission reduction measures and that not considering any measure. We can also see that the gap increases with the increase of MGO price, while the change tendency of the gap is opposite when VLSFO price increases. This is because either the increase of MGO price or the decrease of VLSFO price will increase the price difference between the two types of marine fuels, which will improve the superiority of the model considering the three measures, especially ECAs.

Based on the historical data on the $CO_2$ price, five different carbon taxes, 16, 36, 56, 76, and 96 USD per ton fuel, will be investigated, whose results are reported in Fig. 7. For instances 10-1, 10-2 and 10-3, the gaps between considering and not considering three emission reduction measures decrease with the increase of carbon tax. The main reason is that the ratio of the sum of MGO (marine fuel used within ECAs) price and carbon tax to the sum of VLSFO (marine fuel used outside ECAs) price and carbon tax will decrease (i.e., closer to 1) when the carbon tax increases, so that the optimal path when considering three measures will change to the one closer to the shortest path and the cost savings obtained from path optimization will decrease. In each of the three instances, all ships will be deployed when considering and not considering the three measures under each carbon tax since the total number of available ships is less than the optimal number of ships deployed without considering the limit of ship number. For instances 10-4 and 10-5, the gap may increase or decrease with the increase of carbon tax, due to the change of the optimal number of ships deployed and the decrease of the ratio of the sum of fuel price and carbon tax within ECAs to that outside ECAs. Specifically, when the carbon tax increases from 16 USD per ton fuel to 96 USD per ton fuel, the optimal numbers of ships deployed

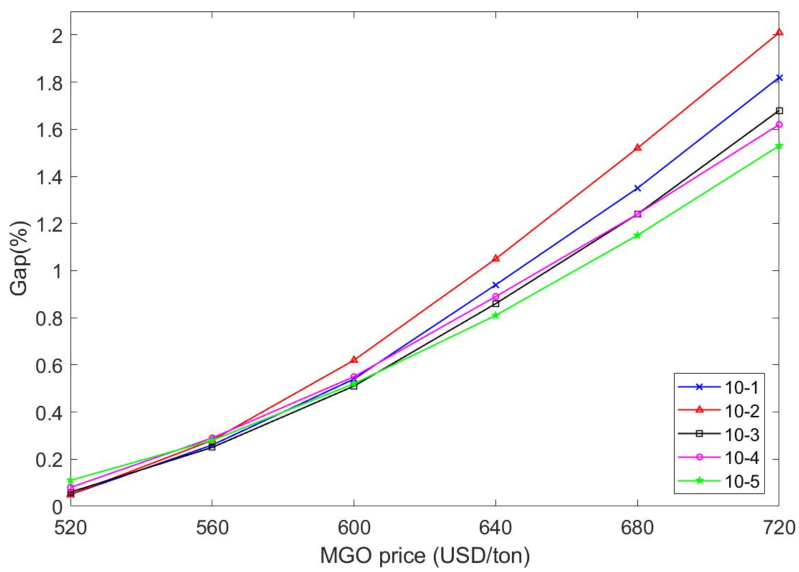


Figure 5: Impact of MGO price on the gap between considering and not considering three emission reduction measures

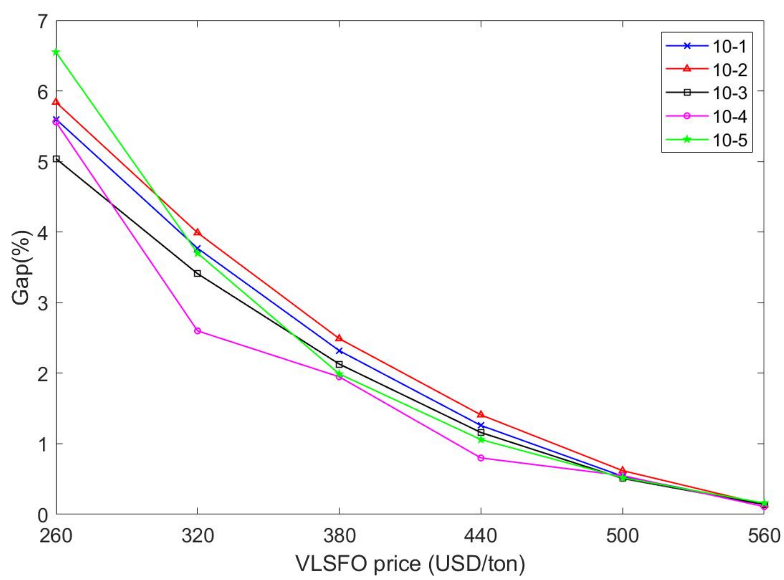


Figure 6: Impact of VLSFO price on the gap between considering and not considering three emission reduction measures

in the cases of considering and not considering the three measures in instance 10-4 are 57 & 57, 58 & 57, 59 & 57, 60 & 57, and 60 & 58, respectively, and the optimal numbers of ships deployed in instance 10-5 are 54 & 53, 54 & 53, 55 & 54, 55 & 54, and 55 & 54, respectively.

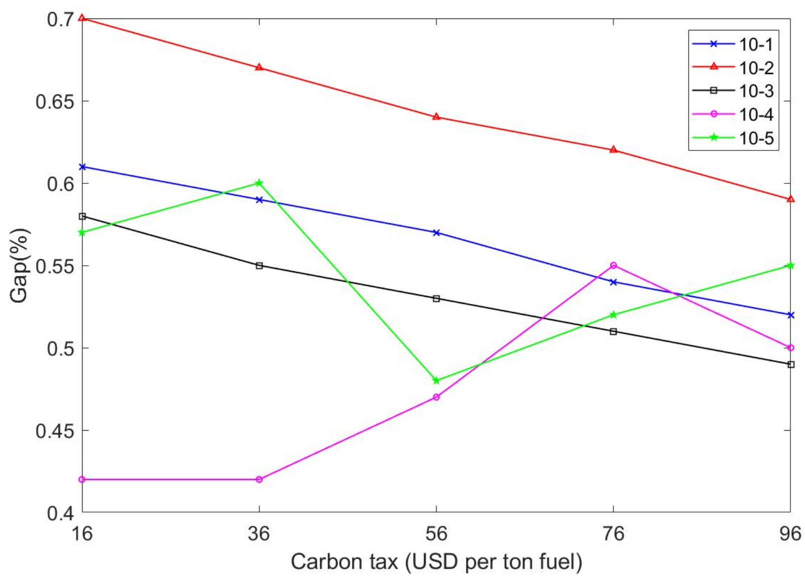


Figure 7: Impact of carbon tax on the gap between considering and not considering three emission reduction measures

## 5. Conclusions

This paper investigates the problem of fleet deployment, sailing path and speed design, and compliance of VSRIPs in a liner shipping company. Three emission reduction measures are simultaneously considered, including sulfur emission regulations, carbon tax, and VSRIPs. We propose a mixed-integer non-linear programming model to minimize the total cost, i.e., fuel cost, carbon tax, and fixed cost, minus dockage refund. We obtain some important properties on the proposed model. For example, the optimal path for a route is fixed when the number of ships deployed is greater than a threshold value; imposing a carbon tax can mitigate the detour of sailing path; the VSRZ group with higher dockage refund has the priority to be complied with when compared to other VSRZ groups with the same VSRZ and ES distances. A tailored algorithm is developed to solve the problem by combining these properties with a dynamic programming approach. On the basis of randomly generated instances from real data, the efficiency of the proposed algorithm is validated by a large number of numerical experiments, and the proposed model is effective in saving operating cost for shipping companies. Our study can provide suggestions on how to design sailing path, sailing speed, and fleet deployment for different liner service routes under the three emission reduction measures.

## Appendix A. Proof of Proposition 1

*Proof.* Without loss of generality, we investigate two super paths $l_1$ and $l_2$ with $d^E_{rl_1} < d^E_{rl_2}$. Suppose that $\tilde{q}_r$ is positive real number in this proposition. Define $q^{\min}_{rl} = \lceil [(d^E_{rl} + d^N_{rl})/V^{\max} + T_r]/T \rceil$ and $\hat{q}_{rl} = \lceil [(\beta d^E_{rl} + d^N_{rl})/V^{\max} + T_r]/T \rceil$.

(i) If $d^E_{rl_1} + d^N_{rl_1} \le d^E_{rl_2} + d^N_{rl_2}$, we define a new super path $l_3$ that satisfies $d^E_{rl_3} + d^N_{rl_3} = d^E_{rl_2} + d^N_{rl_2} \ge d^E_{rl_1} + d^N_{rl_1}$ and $d^E_{rl_3} = d^E_{rl_1}$. Hence, super path $l_1$ is not worse than $l_3$ as $d^E_{rl_1} = d^E_{rl_3}$ and $d^N_{rl_1} \le d^N_{rl_3}$, and $l_3$ is strictly better than $l_2$ since $d^E_{rl_3} < d^E_{rl_2}$ and $d^E_{rl_3} + d^N_{rl_3} = d^E_{rl_2} + d^N_{rl_2}$, indicating that super path $l_1$ is strictly better than $l_2$.

(ii) If $d^E_{rl_1} + d^N_{rl_1} > d^E_{rl_2} + d^N_{rl_2}$ and $\beta d^E_{rl_1} + d^N_{rl_1} \ge \beta d^E_{rl_2} + d^N_{rl_2}$, we have $df(d^E_{rl_1}, d^N_{rl_1}, t^{E*}_r, t^{N*}_r, \tilde{q}_r)/d\tilde{q}_r = -abT(\alpha^N + c^{CO_2}) \cdot (\beta d^E_{rl_1})^{b+1} \cdot (T \cdot \tilde{q}_r - T_r - \frac{d^N_{rl_1}}{V^{\max}})^{-(b+1)}$ when $q^{\min}_{rl_1} \le \tilde{q}_r < \hat{q}_{rl_1}$, and we also observe that $df(d^E_{rl_2}, d^N_{rl_2}, t^{E*}_r, t^{N*}_r, \tilde{q}_r)/d\tilde{q}_r = -abT(\alpha^N + c^{CO_2}) \cdot (\beta d^E_{rl_2})^{b+1} \cdot (T \cdot \tilde{q}_r - T_r - \frac{d^N_{rl_2}}{V^{\max}})^{-(b+1)}$ when $q^{\min}_{rl_2} \le \tilde{q}_r < \hat{q}_{rl_2}$ and $df(d^E_{rl_2}, d^N_{rl_2}, t^{E*}_r, t^{N*}_r, \tilde{q}_r)/d\tilde{q}_r = -abT(\alpha^N + c^{CO_2}) \cdot (\beta d^E_{rl_2} + d^N_{rl_2})^{b+1} \cdot (T \cdot \tilde{q}_r - T_r)^{-(b+1)}$ when $\tilde{q}_r \ge \hat{q}_{rl_2}$. It is derived that $\beta d^E_{rl_1}/(T \cdot \tilde{q}_r - T_r - \frac{d^N_{rl_1}}{V^{\max}}) > \beta d^E_{rl_2}/(T \cdot \tilde{q}_r - T_r - \frac{d^N_{rl_2}}{V^{\max}})$ when $q^{\min}_{rl_1} \le \tilde{q}_r < \hat{q}_{rl_2}$ because $(\beta d^E_{rl_1} + d^N_{rl_1})/(T\tilde{q}_r - T_r) > (\beta d^E_{rl_2} + d^N_{rl_2})/(T\tilde{q}_r - T_r) > V^{\max}$ and $d^N_{rl_1} > d^N_{rl_2}$ and that $\beta d^E_{rl_1}/(T \cdot \tilde{q}_r - T_r - \frac{d^N_{rl_1}}{V^{\max}}) > V^{\max} > (\beta d^E_{rl_2} + d^N_{rl_2})/(T \cdot \tilde{q}_r - T_r)$ when $\hat{q}_{rl_2} \le \tilde{q}_r \le \hat{q}_{rl_1}$. We then obtain that $df(d^E_{rl_1}, d^N_{rl_1}, t^{E*}_r, t^{N*}_r, \tilde{q}_r)/d\tilde{q}_r < df(d^E_{rl_2}, d^N_{rl_2}, t^{E*}_r, t^{N*}_r, \tilde{q}_r)/d\tilde{q}_r$ when $q^{\min}_{rl_1} \le \tilde{q}_r \le \hat{q}_{rl_1}$, and we also have $f(d^E_{rl_1}, d^N_{rl_1}, t^{E*}_r, t^{N*}_r, \tilde{q}_r) > f(d^E_{rl_2}, d^N_{rl_2}, t^{E*}_r, t^{N*}_r, \tilde{q}_r)$ when $\tilde{q}_r \ge \hat{q}_{rl_1}$. Hence, $f(d^E_{rl_1}, d^N_{rl_1}, t^{E*}_r, t^{N*}_r, \tilde{q}_r)$ is always greater than $f(d^E_{rl_2}, d^N_{rl_2}, t^{E*}_r, t^{N*}_r, \tilde{q}_r)$ when $\tilde{q}_r \ge q^{\min}_{rl_1}$.

(iii) If $d^E_{rl_1} + d^N_{rl_1} > d^E_{rl_2} + d^N_{rl_2}$ and $\beta d^E_{rl_1} + d^N_{rl_1} < \beta d^E_{rl_2} + d^N_{rl_2}$, the superiority of super path is dependent on $\tilde{q}_r$. We will take an example by setting the parameters below: $\alpha^E = 600$, $\alpha^N = 500$, $c^{CO_2} = 76$, $a = 0.00047$, $b = 2.118$, $V^{\max} = 25$, $T_r = 0$, $d^E_{rl_1} = 4,800$,

$d^N_{rl_1} = 20,300$, $d^E_{rl_2} = 5,800$, and $d^N_{rl_2} = 19,248$. Hence, we have $f(d^E_{rl_1}, d^N_{rl_1}, t^{E*}_r, t^{N*}_r, 6) = 6,355,731 > f(d^E_{rl_2}, d^N_{rl_2}, t^{E*}_r, t^{N*}_r, 6) = 6,355,584$ and $f(d^E_{rl_1}, d^N_{rl_1}, t^{E*}_r, t^{N*}_r, 7) = 4,583,051 < f(d^E_{rl_2}, d^N_{rl_2}, t^{E*}_r, t^{N*}_r, 7) = 4,583,436$, i.e., super path $l_2$ can lead to lower cost when $\tilde{q}_r = 6$, while $l_1$ is better when $\tilde{q}_r = 7$. Therefore, this proposition is proved. □

## Appendix B. Proof of Proposition 3

*Proof.* (i) We analyze a route $r$ with $\Omega$ ES ports that include VSRZs with the same radius (recorded as $d'_r$), which are denoted by $p^{[1]}, ..., p^{[\Omega]}$ in decreasing order of the refunds of these VSRZs (recorded as $c^{ref'}_{rp^{[1]}} \geq ... \geq c^{ref'}_{rp^{[\Omega]}}$). Super path $l$ with the sailing distances within and outside ECAs $d^E_{rl}$ and $d^N_{rl}$ is chosen. The compliance for VSRZ $j \in J_{rp}$ at port $p \in P^S_r \cup P^{ES}_r$ of route $r \in R$ is $y'_{rpj}$ ($y'_r$ is all vectors of $y'_{rpj}$, $p \in P^S_r \cup P^{ES}_r$, $j \in J_{rp}$), and $y'_{rpj} = 0$ for all $p = p^{[1]}, ..., p^{[\Omega]}$ and $j \in J_{rp}$. We also define $D^{ES'}_r = \sum_{p \in P^{ES}_r} \sum_{j \in J_{rp}} 2d_{rpj} y'_{rpj}$ and $D^{S'}_r = \sum_{p \in P^S_r} \sum_{j \in J_{rp}} 2d_{rpj} y'_{rpj}$. Since all VSRIPs at ES ports will be complied with in the optimal solution when $\tilde{q}_r \geq \hat{q}^{ES'}_{rl}$, we only consider the case of $\tilde{q}_r < \hat{q}^{ES'}_{rl}$, where $\hat{q}^{ES'}_{rl} = \left\lceil [\beta d^E_{rl} + (d^N_{rl} - D^{S'}_r) + \beta T_r V^S + \beta D^{S'}_r] / (\beta T \cdot V^S) \right\rceil$.

If the company chooses a VSRZ with the radius $d'_r$ at ES port $\omega$ among the $\Omega$ ES ports whose speed limit will be complied with, the compliance of VSRZs $y'_r$ is changed to $y''_r$ with the only difference $y''_{rp^{[\omega]}j} = 1$ when $d_{rp^{[\omega]}j} = d'_r$. The difference between the minimum cost for route $r$ with the compliance of VSRZs $y''_r$ and that with $y'_r$ is

$$
\begin{aligned}
& g^{dif}(d^E_{rl}, d^N_{rl}, t^{E*}_r, t^{S*}_r, t^{ES*}_r, t^{N*}_r, \tilde{q}_r, y'_r, y''_r) \\
&= \begin{cases}
(\alpha^E + c^{CO_2})[(d^E_{rl} - D^{ES'}_r - 2d'_r)^{b+1} \cdot a(T \cdot q_r - T_r - \frac{d^N_{rl} - D^{S'}_r}{V^{\max}} - \frac{D^{ES'}_r + D^{S'}_r + 2d'_r}{V^S})^{-b} & \\
-(d^E_{rl} - D^{ES'}_r)^{b+1} \cdot a(T \cdot q_r - T_r - \frac{d^N_{rl} - D^{S'}_r}{V^{\max}} - \frac{D^{ES'}_r + D^{S'}_r}{V^S})^{-b} + 2d'_r \cdot a(V^S)^b] - c^{ref'}_{rp^{[\omega]}}, & q^{\min}_{rl} \leq \tilde{q}_r < \hat{q}^{E'}_{rl} \\
(\alpha^E + c^{CO_2})[(d^E_{rl} - D^{ES'}_r - 2d'_r)^{b+1} \cdot a(T \cdot q_r - T_r - \frac{d^N_{rl} - D^{S'}_r}{V^{\max}} - \frac{D^{ES'}_r + D^{S'}_r + 2d'_r}{V^S})^{-b} & \\
+2d'_r \cdot a(V^S)^b] - (\alpha^N + c^{CO_2})\{[\beta(d^E_{rl} - D^{ES'}_r) + (d^N_{rl} - D^{S'}_r)]^{b+1} \cdot a(T \cdot q_r - T_r - \frac{D^{ES'}_r + D^{S'}_r}{V^S})^{-b} & \\
-(d^N_{rl} - D^{S'}_r) a(V^{\max})^b\} - c^{ref'}_{rp^{[\omega]}}, & \hat{q}^{E'}_{rl} \leq \tilde{q}_r < \hat{q}^{E''}_{rl} \\
(\alpha^N + c^{CO_2})\{[\beta(d^E_{rl} - D^{ES'}_r - 2d'_r) + (d^N_{rl} - D^{S'}_r)]^{b+1} \cdot a(T \cdot q_r - T_r - \frac{D^{ES'}_r + D^{S'}_r + 2d'_r}{V^S})^{-b} & \\
-[\beta(d^E_{rl} - D^{ES'}_r) + (d^N_{rl} - D^{S'}_r)]^{b+1} \cdot a(T \cdot q_r - T_r - \frac{D^{ES'}_r + D^{S'}_r}{V^S})^{-b}\} & \\
+(\alpha^E + c^{CO_2}) \cdot 2d'_r \cdot a(V^S)^b - c^{ref'}_{rp^{[\omega]}}, & \hat{q}^{E''}_{rl} \leq \tilde{q}_r < \hat{q}^{ES'}_{rl},
\end{cases}
\end{aligned}
\tag{B.1}
$$

where $q_{rl}^{\min} = \left\lceil [(d_{rl}^E - D_r^{ES'})V^S + (d_{rl}^N - D_r^{S'})V^S + T_r V^{\max} V^S + (D_r^{ES'} + D_r^{S'})V^{\max}]/(T \cdot V^{\max} V^S) \right\rceil$, $\hat{q}_{rl}^{E'} = \left\lceil [\beta(d_{rl}^E - D_r^{ES'})V^S + (d_{rl}^N - D_r^{S'})V^S + T_r V^{\max} V^S + (D_r^{ES'} + D_r^{S'})V^{\max}]/(T \cdot V^{\max} V^S) \right\rceil$ and $\hat{q}_{rl}^{E''} = \left\lceil [\beta(d_{rl}^E - D_r^{ES'} - 2d'_r)V^S + (d_{rl}^N - D_r^{S'})V^S + T_r V^{\max} V^S + (D_r^{ES'} + D_r^{S'} + 2d'_r)V^{\max}]/(T \cdot V^{\max} V^S) \right\rceil$. Eq. (B.1) shows that the dockage refund is the only difference for all choices of VSRZs with the radius $d'_r$ at the $\Omega$ ES ports, and therefore the VSRZ with the highest dockage refund will be chosen for reducing cost.

(ii) This finding can be proved by the similar method in (i). □

## Appendix C. Proof of Proposition 4

*Proof.* Focusing on the situation of $\tilde{q}_r \geq \hat{q}_r^{E,\max}$, we will prove this finding by contradiction. Referring to Eq. (18), the super path with the minimum $\beta d_{rl}^E + d_{rl}^N$ for all $l \in L_r$ is the optimal one for a route $r$ only including ECA and non-ES ports when $\tilde{q}_r \geq \hat{q}_r^{E,\max}$. For a route $r$ with all types of ports, we assume that the compliance for VSRZ $j \in J_{rp}$ at port $p \in P_r^S \cup P_r^{ES}$ of route $r \in R$ is $\tilde{y}_{rpj}$ ($\tilde{y}_r$ is all vectors of $\tilde{y}_{rpj}$, $p \in P_r^S \cup P_r^{ES}$, $j \in J_{rp}$), and we have $\tilde{D}_r^{ES} = \sum_{p \in P_r^{ES}} \sum_{j \in J_{rp}} 2d_{rpj}\tilde{y}_{rpj}$, $\tilde{D}_r^S = \sum_{p \in P_r^S} \sum_{j \in J_{rp}} 2d_{rpj}\tilde{y}_{rpj}$, and $\tilde{C}_r^{ref} = \sum_{p \in P_r^S \cup P_r^{ES}} \sum_{j \in J_{rp}} c_{rpj}^{ref} \tilde{y}_{rpj}$. We also assume that there exists a super path $\tilde{l}$ which can lead to the lower cost than the super path $l^*$ with the compliance $\tilde{y}_r$.

Referring to Eqs. (20), (21), and (22), there are three cases as follows.

(i) For the case of $(\beta d_{rl^*}^E + d_{rl^*}^N)/(T \cdot \tilde{q}_r - T_r) \leq V^S$, the cost including fuel cost and carbon tax minus dockage refund for super path $l^*$ is $(\alpha^N + c^{CO_2})(\beta d_{rl^*}^E + d_{rl^*}^N)^{b+1} \cdot a(T \cdot \tilde{q}_r - T_r)^{-b} - \tilde{C}_r^{ref}$. If $(\beta d_{r\tilde{l}}^E + d_{r\tilde{l}}^N)/(T \cdot q_r - T_r) \leq V^S$, then the cost of super path $l^*$ is no more than the cost of super path $\tilde{l}$, i.e., $(\alpha^N + c^{CO_2})(\beta d_{r\tilde{l}}^E + d_{r\tilde{l}}^N)^{b+1} \cdot a(T \cdot \tilde{q}_r - T_r)^{-b} - \tilde{C}_r^{ref}$, since $\beta d_{rl^*}^E + d_{rl^*}^N \leq \beta d_{r\tilde{l}}^E + d_{r\tilde{l}}^N$; if $V^S < (\beta d_{r\tilde{l}}^E + d_{r\tilde{l}}^N - \tilde{D}_r^S)/(T \cdot q_r - T_r - \tilde{D}_r^S/V^S) \leq \beta V^S$, then $(\alpha^N + c^{CO_2})(\beta d_{rl^*}^E + d_{rl^*}^N)^{b+1} \cdot a(T \cdot \tilde{q}_r - T_r)^{-b} - \tilde{C}_r^{ref} < (\alpha^N + c^{CO_2})[\beta d_{r\tilde{l}}^E + (d_{r\tilde{l}}^N - \tilde{D}_r^S)]^{b+1} \cdot a(T \cdot \tilde{q}_r - T_r - \frac{\tilde{D}_r^S}{V^S})^{-b} + (\alpha^N + c^{CO_2})\tilde{D}_r^S \cdot a(V^S)^b - \tilde{C}_r^{ref}$ because $[\beta d_{r\tilde{l}}^E + (d_{r\tilde{l}}^N - \tilde{D}_r^S)]/(T \cdot \tilde{q}_r - T_r - \tilde{D}_r^S/V^S) > V^S > (\beta d_{rl^*}^E + d_{rl^*}^N)/(T \cdot q_r - T_r)$; if $\beta V^S < [\beta(d_{r\tilde{l}}^E - \tilde{D}_r^{ES}) + d_{r\tilde{l}}^N - \tilde{D}_r^S]/[T \cdot q_r - T_r - (\tilde{D}_r^{ES} + \tilde{D}_r^S)/V^S] \leq V^{\max}$, then $(\alpha^N + c^{CO_2})(\beta d_{rl^*}^E + d_{rl^*}^N)^{b+1} \cdot a(T \cdot \tilde{q}_r - T_r)^{-b} - \tilde{C}_r^{ref} < (\alpha^N + c^{CO_2})[\beta(d_{r\tilde{l}}^E - \tilde{D}_r^{ES}) + (d_{r\tilde{l}}^N - \tilde{D}_r^S)]^{b+1} \cdot a(T \cdot \tilde{q}_r - T_r - \frac{\tilde{D}_r^{ES} + \tilde{D}_r^S}{V^S})^{-b} + [(\alpha^E + c^{CO_2})\tilde{D}_r^{ES} + (\alpha^N + c^{CO_2})\tilde{D}_r^S] \cdot a(V^S)^b - \tilde{C}_r^{ref}$.

(ii) For the case of $V^S < (\beta d_{rl^*}^E + d_{rl^*}^N - \tilde{D}_r^S)/(T \cdot \tilde{q}_r - T_r - \tilde{D}_r^S/V^S) \leq \beta V^S$, we have $(\beta d_{r\tilde{l}}^E + d_{r\tilde{l}}^N - \tilde{D}_r^S)/(T \cdot q_r - T_r - \tilde{D}_r^S/V^S) \geq (\beta d_{rl^*}^E + d_{rl^*}^N - \tilde{D}_r^S)/(T \cdot q_r - T_r - \tilde{D}_r^S/V^S)$. We derive that $(\alpha^N+c^{CO_2})[\beta d^E_{rl^*}+(d^N_{rl^*}-\tilde{D}^S_r)]^{b+1}\cdot a(T\cdot\tilde{q}_r-T_r-\frac{\tilde{D}^S_r}{V^S})^{-b}+(\alpha^N+c^{CO_2})\tilde{D}^S_r\cdot a(V^S)^b-\tilde{C}^{ref}_r \le (\alpha^N+c^{CO_2})[\beta d^E_{r\tilde{l}}+(d^N_{r\tilde{l}}-\tilde{D}^S_r)]^{b+1}\cdot a(T\cdot\tilde{q}_r-T_r-\frac{\tilde{D}^S_r}{V^S})^{-b}+(\alpha^N+c^{CO_2})\tilde{D}^S_r\cdot a(V^S)^b-\tilde{C}^{ref}_r$ when $V^S<(\beta d^E_{r\tilde{l}}+d^N_{r\tilde{l}}-\tilde{D}^S_r)/(T\cdot q_r-T_r-\tilde{D}^S_r/V^S)\le \beta V^S$ and $(\alpha^N+c^{CO_2})[\beta d^E_{rl^*}+(d^N_{rl^*}-\tilde{D}^S_r)]^{b+1}\cdot a(T\cdot\tilde{q}_r-T_r-\frac{\tilde{D}^S_r}{V^S})^{-b}+(\alpha^N+c^{CO_2})\tilde{D}^S_r\cdot a(V^S)^b-\tilde{C}^{ref}_r<(\alpha^N+c^{CO_2})[\beta(d^E_{r\tilde{l}}-\tilde{D}^{ES}_r)+(d^N_{r\tilde{l}}-\tilde{D}^S_r)]^{b+1}\cdot a(T\cdot\tilde{q}_r-T_r-\frac{\tilde{D}^{ES}_r+\tilde{D}^S_r}{V^S})^{-b}+[(\alpha^E+c^{CO_2})\tilde{D}^{ES}_r+(\alpha^N+c^{CO_2})\tilde{D}^S_r]\cdot a(V^S)^b-\tilde{C}^{ref}_r$ when $\beta V^S<[\beta(d^E_{r\tilde{l}}-\tilde{D}^{ES}_r)+d^N_{r\tilde{l}}-\tilde{D}^S_r]/[T\cdot\tilde{q}_r-T_r-(\tilde{D}^{ES}_r+\tilde{D}^S_r)/V^S]\le V^{\max}$.

(iii) For the case of $\beta V^S<[\beta(d^E_{rl^*}-\tilde{D}^{ES}_r)+d^N_{rl^*}-\tilde{D}^S_r]/[T\cdot\tilde{q}_r-T_r-(\tilde{D}^{ES}_r+\tilde{D}^S_r)/V^S]\le V^{\max}$, we have $[\beta(d^E_{r\tilde{l}}-\tilde{D}^{ES}_r)+d^N_{r\tilde{l}}-\tilde{D}^S_r]/[T\cdot\tilde{q}_r-T_r-(\tilde{D}^{ES}_r+\tilde{D}^S_r)/V^S]\ge[\beta(d^E_{rl^*}-\tilde{D}^{ES}_r)+d^N_{rl^*}-\tilde{D}^S_r]/[T\cdot\tilde{q}_r-T_r-(\tilde{D}^{ES}_r+\tilde{D}^S_r)/V^S]$, and we obtain that $(\alpha^N+c^{CO_2})[\beta(d^E_{rl^*}-\tilde{D}^{ES}_r)+(d^N_{rl^*}-\tilde{D}^S_r)]^{b+1}\cdot a(T\cdot\tilde{q}_r-T_r-\frac{\tilde{D}^{ES}_r+\tilde{D}^S_r}{V^S})^{-b}+[(\alpha^E+c^{CO_2})\tilde{D}^{ES}_r+(\alpha^N+c^{CO_2})\tilde{D}^S_r]\cdot a(V^S)^b-\tilde{C}^{ref}_r\le(\alpha^N+c^{CO_2})[\beta(d^E_{r\tilde{l}}-\tilde{D}^{ES}_r)+(d^N_{r\tilde{l}}-\tilde{D}^S_r)]^{b+1}\cdot a(T\cdot\tilde{q}_r-T_r-\frac{\tilde{D}^{ES}_r+\tilde{D}^S_r}{V^S})^{-b}+[(\alpha^E+c^{CO_2})\tilde{D}^{ES}_r+(\alpha^N+c^{CO_2})\tilde{D}^S_r]\cdot a(V^S)^b-\tilde{C}^{ref}_r$.

In summary, super path $\tilde{l}$ with lower cost than super path $l^*$ does not exist for any compliance of VSRZs $\tilde{y}_r$, and thus it is concluded that super path $l^*$ is always the optimal one when $\tilde{q}_r\ge\hat{q}^{E,\max}_r$. □

## Appendix D. Proof of Proposition 5

*Proof.* This finding will be proved by contradiction. Denote by $l^*$ the optimal super path when the carbon tax is considered and $l^{*'}$ the optimal one when the carbon tax is not applied. Assume $d^E_{rl^*}+d^N_{rl^*}>d^E_{rl^{*'}}+d^N_{rl^{*'}}$. It is easy to derive that $d^E_{rl^*}<d^E_{rl^{*'}}$ and $\beta d^E_{rl^*}+d^N_{rl^*}<\beta d^E_{rl^{*'}}+d^N_{rl^{*'}}$ by referring to Proposition 1. Suppose that the compliance of VSRZs is $\tilde{y}_r$. Define $\beta'=(\alpha^E/\alpha^N)^{1/(b+1)}$ and for super path $l$, $q^{\min}_{rl}=\left\lceil[(d^E_{rl}-\tilde{D}^{ES}_r)V^S+(d^N_{rl}-\tilde{D}^S_r)V^S+T_rV^{\max}V^S+(\tilde{D}^{ES}_r+\tilde{D}^S_r)V^{\max}]/(T\cdot V^{\max}V^S)\right\rceil$, $\hat{q}^E_{rl}=\left\lceil[\beta(d^E_{rl}-\tilde{D}^{ES}_r)V^S+(d^N_{rl}-\tilde{D}^S_r)V^S+T_rV^{\max}V^S+(\tilde{D}^{ES}_r+\tilde{D}^S_r)V^{\max}]/(T\cdot V^{\max}V^S)\right\rceil$, $(\hat{q}^E_{rl})'=\left\lceil[\beta'(d^E_{rl}-\tilde{D}^{ES}_r)V^S+(d^N_{rl}-\tilde{D}^S_r)V^S+T_rV^{\max}V^S+(\tilde{D}^{ES}_r+\tilde{D}^S_r)V^{\max}]/(T\cdot V^{\max}V^S)\right\rceil$, and $\hat{q}^{ES}_{rl}=\left\lceil[\beta d^E_{rl}+(d^N_{rl}-\tilde{D}^S_r)+\beta T_rV^S+\beta\tilde{D}^S_r]/(\beta T\cdot V^S)\right\rceil$. We also define the cost function including fuel cost minus dockage refund without carbon tax for super path $l$ $g'(d^E_{rl},d^N_{rl},t^{E*}_r,t^{S*}_r,t^{ES*}_r,t^{N*}_r,\tilde{q}_r,\tilde{y}_r)=\alpha^E[(d^E_{rl}-\tilde{D}^{ES}_r)^{b+1}a(T\cdot\tilde{q}_r-T_r-\frac{d^N_{rl}-\tilde{D}^S_r}{V^{\max}}-\frac{\tilde{D}^{ES}_r+\tilde{D}^S_r}{V^S})^{-b}+\tilde{D}^{ES}_r\cdot a(V^S)^b]+\alpha^N[(d^N_{rl}-\tilde{D}^S_r)\cdot a(V^{\max})^b+\tilde{D}^S_r\cdot a(V^S)^b]-\tilde{C}^{ref}_r$ when $q^{\min}_{rl}\le\tilde{q}_r<(\hat{q}^E_{rl})'$ and $g'(d^E_{rl},d^N_{rl},t^{E*}_r,t^{S*}_r,t^{ES*}_r,t^{N*}_r,\tilde{q}_r,\tilde{y}_r)=\alpha^N[\beta'(d^E_{rl}-\tilde{D}^{ES}_r)+(d^N_{rl}-$

$\tilde{D}_r^S)]^{b+1} \cdot a(T \cdot \tilde{q}_r - T_r - \frac{\tilde{D}_r^{ES}+\tilde{D}_r^S}{V^S})^{-b} + [\alpha^E \tilde{D}_r^{ES} + \alpha^N \tilde{D}_r^S] \cdot a(V^S)^b - \tilde{C}_r^{ref}$ when $(\hat{q}_{rl}^E)' \leq \tilde{q}_r < \hat{q}_{rl}^{ES}$. The cost functions should satisfy that $g(d_{rl^*}^E, d_{rl^*}^N, t_r^{E*}, t_r^{S*}, t_r^{ES*}, t_r^{N*}, \tilde{q}_r, \tilde{y}_r) < g(d_{rl^{*\prime}}^E, d_{rl^{*\prime}}^N, t_r^{E*}, t_r^{S*}, t_r^{ES*}, t_r^{N*}, \tilde{q}_r, \tilde{y}_r)$ and $g'(d_{rl^*}^E, d_{rl^*}^N, t_r^{E*}, t_r^{S*}, t_r^{ES*}, t_r^{N*}, \tilde{q}_r, \tilde{y}_r) > g'(d_{rl^{*\prime}}^E, d_{rl^{*\prime}}^N, t_r^{E*}, t_r^{S*}, t_r^{ES*}, t_r^{N*}, \tilde{q}_r, \tilde{y}_r)$. We only consider the situation of $q_{rl^*}^{\min} < \hat{q}_{rl^*}^E < \hat{q}_{rl^{*\prime}}^E < (\hat{q}_{rl^*}^E)' < (\hat{q}_{rl^{*\prime}}^E)' < \hat{q}_{rl^{*\prime}}^{ES}$ for simplification. The other situations can be analyzed by the similar method and the same result can be obtained.

Assuming that $\tilde{q}_r$ can take fractions, we analyze five cases on $\tilde{q}_r$ in the situation $q_{rl^*}^{\min} < \hat{q}_{rl^*}^E < \hat{q}_{rl^{*\prime}}^E < (\hat{q}_{rl^*}^E)' < (\hat{q}_{rl^{*\prime}}^E)' < \hat{q}_{rl^{*\prime}}^{ES}$.

(i) When $\tilde{q}_r \geq (\hat{q}_{rl^{*\prime}}^E)'$, we can obtain $\beta' d_{rl^{*\prime}}^E + d_{rl^{*\prime}}^N - (\beta' d_{rl^*}^E + d_{rl^*}^N) = [\beta d_{rl^{*\prime}}^E + d_{rl^{*\prime}}^N - (\beta d_{rl^*}^E + d_{rl^*}^N)] + [(\beta' - \beta) d_{rl^{*\prime}}^E - (\beta' - \beta) d_{rl^*}^E] > 0$, meaning $l^{*\prime}$ is not the optimal path when there is no carbon tax.

(ii) When $(\hat{q}_{rl^*}^E)' \leq \tilde{q}_r < (\hat{q}_{rl^{*\prime}}^E)'$, the first-order derivatives of the cost functions without considering carbon tax in $\tilde{q}_r$ for super paths $l^*$ and $l^{*\prime}$ are $dg'(d_{rl^*}^E, d_{rl^*}^N, t_r^{E*}, t_r^{S*}, t_r^{ES*}, t_r^{N*}, \tilde{q}_r, \tilde{y}_r)/d\tilde{q}_r = -\alpha^N abT[\beta'(d_{rl^*}^E - \tilde{D}_r^{ES}) + (d_{rl^*}^N - \tilde{D}_r^S)]^{b+1}(T \cdot \tilde{q}_r - T_r - \frac{\tilde{D}_r^{ES}+\tilde{D}_r^S}{V^S})^{-(b+1)}$ and $dg'(d_{rl^{*\prime}}^E, d_{rl^{*\prime}}^N, t_r^{E*}, t_r^{S*}, t_r^{ES*}, t_r^{N*}, \tilde{q}_r, \tilde{y}_r)/d\tilde{q}_r = -\alpha^N abT[\beta'(d_{rl^{*\prime}}^E - \tilde{D}_r^{ES})]^{b+1}(T \cdot \tilde{q}_r - T_r - \frac{d_{rl^{*\prime}}^N - \tilde{D}_r^S}{V^{\max}} - \frac{\tilde{D}_r^{ES}+\tilde{D}_r^S}{V^S})^{-(b+1)}$, respectively, and we observe that $dg'(d_{rl^*}^E, d_{rl^*}^N, t_r^{E*}, t_r^{S*}, t_r^{ES*}, t_r^{N*}, \tilde{q}_r, \tilde{y}_r)/d\tilde{q}_r > dg'(d_{rl^{*\prime}}^E, d_{rl^{*\prime}}^N, t_r^{E*}, t_r^{S*}, t_r^{ES*}, t_r^{N*}, \tilde{q}_r, \tilde{y}_r)/d\tilde{q}_r$ since $[\beta'(d_{rl^*}^E - \tilde{D}_r^{ES}) + (d_{rl^*}^N - \tilde{D}_r^S)]/(T \cdot \tilde{q}_r - T_r - \frac{\tilde{D}_r^{ES}+\tilde{D}_r^S}{V^S}) < V^{\max} < [\beta'(d_{rl^{*\prime}}^E - \tilde{D}_r^{ES})]/(T \cdot \tilde{q}_r - T_r - \frac{d_{rl^{*\prime}}^N - \tilde{D}_r^S}{V^{\max}} - \frac{\tilde{D}_r^{ES}+\tilde{D}_r^S}{V^S})$. We also have $g'(d_{rl^*}^E, d_{rl^*}^N, t_r^{E*}, t_r^{S*}, t_r^{ES*}, t_r^{N*}, (\hat{q}_{rl^{*\prime}}^E)', \tilde{y}_r) < g'(d_{rl^{*\prime}}^E, d_{rl^{*\prime}}^N, t_r^{E*}, t_r^{S*}, t_r^{ES*}, t_r^{N*}, (\hat{q}_{rl^{*\prime}}^E)', \tilde{y}_r)$. Therefore, it is concluded that $g'(d_{rl^*}^E, d_{rl^*}^N, t_r^{E*}, t_r^{S*}, t_r^{ES*}, t_r^{N*}, \tilde{q}_r, \tilde{y}_r) < g'(d_{rl^{*\prime}}^E, d_{rl^{*\prime}}^N, t_r^{E*}, t_r^{S*}, t_r^{ES*}, t_r^{N*}, \tilde{q}_r, \tilde{y}_r)$ when $(\hat{q}_{rl^*}^E)' \leq \tilde{q}_r < (\hat{q}_{rl^{*\prime}}^E)'$.

(iii) When $\hat{q}_{rl^{*\prime}}^E \leq \tilde{q}_r < (\hat{q}_{rl^*}^E)'$, we have $dg'(d_{rl^*}^E, d_{rl^*}^N, t_r^{E*}, t_r^{S*}, t_r^{ES*}, t_r^{N*}, \tilde{q}_r, \tilde{y}_r)/d\tilde{q}_r = -\alpha^E abT \frac{1}{\beta^{b+1}}[\beta(d_{rl^*}^E - \tilde{D}_r^{ES})]^{b+1}(T \cdot \tilde{q}_r - T_r - \frac{d_{rl^*}^N - \tilde{D}_r^S}{V^{\max}} - \frac{\tilde{D}_r^{ES}+\tilde{D}_r^S}{V^S})^{-(b+1)}$ and $dg'(d_{rl^{*\prime}}^E, d_{rl^{*\prime}}^N, t_r^{E*}, t_r^{S*}, t_r^{ES*}, t_r^{N*}, \tilde{q}_r, \tilde{y}_r)/d\tilde{q}_r = -\alpha^E abT \frac{1}{\beta^{b+1}}[\beta(d_{rl^{*\prime}}^E - \tilde{D}_r^{ES})]^{b+1}(T \cdot \tilde{q}_r - T_r - \frac{d_{rl^{*\prime}}^N - \tilde{D}_r^S}{V^{\max}} - \frac{\tilde{D}_r^{ES}+\tilde{D}_r^S}{V^S})^{-(b+1)}$. We find that $[\beta(d_{rl^*}^E - \tilde{D}_r^{ES})]/(T \cdot \tilde{q}_r - T_r - \frac{d_{rl^*}^N - \tilde{D}_r^S}{V^{\max}} - \frac{\tilde{D}_r^{ES}+\tilde{D}_r^S}{V^S}) < [\beta(d_{rl^{*\prime}}^E - \tilde{D}_r^{ES})]/(T \cdot \tilde{q}_r - T_r - \frac{d_{rl^{*\prime}}^N - \tilde{D}_r^S}{V^{\max}} - \frac{\tilde{D}_r^{ES}+\tilde{D}_r^S}{V^S}) < V^{\max}$ as $\beta d_{rl^*}^E + d_{rl^*}^N < \beta d_{rl^{*\prime}}^E + d_{rl^{*\prime}}^N$,

$d^N_{rl^*} > d^N_{rl^{*\prime}}$ and the sailing speed outside ECAs is $V^{\max}$, and thus $dg'(d^E_{rl^*}, d^N_{rl^*}, t^{E*}_r, t^{S*}_r, t^{ES*}_r, t^{N*}_r, \tilde{q}_r, \tilde{y}_r)/d\tilde{q}_r > dg'(d^E_{rl^{*\prime}}, d^N_{rl^{*\prime}}, t^{E*}_r, t^{S*}_r, t^{ES*}_r, t^{N*}_r, \tilde{q}_r, \tilde{y}_r)/d\tilde{q}_r$. Combined with the result in (ii) of this proposition, the analysis in (iii) shows that $g'(d^E_{rl^{*\prime}}, d^N_{rl^{*\prime}}, t^{E*}_r, t^{S*}_r, t^{ES*}_r, t^{N*}_r, \tilde{q}_r, \tilde{y}_r)$ must be greater than $g'(d^E_{rl^*}, d^N_{rl^*}, t^{E*}_r, t^{S*}_r, t^{ES*}_r, t^{N*}_r, \tilde{q}_r, \tilde{y}_r)$ in the case of $\hat{q}^E_{rl^{*\prime}} \le \tilde{q}_r < (\hat{q}^E_{rl^*})'$.

(iv) When $\hat{q}^E_{rl^*} \le \tilde{q}_r < \hat{q}^E_{rl^{*\prime}}$, the first-order derivatives are still $dg'(d^E_{rl^*}, d^N_{rl^*}, t^{E*}_r, t^{S*}_r, t^{ES*}_r, t^{N*}_r, \tilde{q}_r, \tilde{y}_r)/d\tilde{q}_r = -\alpha^E abT\frac{1}{\beta^{b+1}}[\beta(d^E_{rl^*} - \tilde{D}^{ES}_r)]^{b+1}(T \cdot \tilde{q}_r - T_r - \frac{d^N_{rl^*} - \tilde{D}^S_r}{V^{\max}} - \frac{\tilde{D}^{ES}_r + \tilde{D}^S_r}{V^S})^{-(b+1)}$ and $dg'(d^E_{rl^{*\prime}}, d^N_{rl^{*\prime}}, t^{E*}_r, t^{S*}_r, t^{ES*}_r, t^{N*}_r, \tilde{q}_r, \tilde{y}_r)/d\tilde{q}_r = -\alpha^E abT\frac{1}{\beta^{b+1}}[\beta(d^E_{rl^{*\prime}} - \tilde{D}^{ES}_r)]^{b+1}(T \cdot \tilde{q}_r - T_r - \frac{d^N_{rl^{*\prime}} - \tilde{D}^S_r}{V^{\max}} - \frac{\tilde{D}^{ES}_r + \tilde{D}^S_r}{V^S})^{-(b+1)}$. It is derived that $[\beta(d^E_{rl^*} - \tilde{D}^{ES}_r)]/(T \cdot \tilde{q}_r - T_r - \frac{d^N_{rl^*} - \tilde{D}^S_r}{V^{\max}} - \frac{\tilde{D}^{ES}_r + \tilde{D}^S_r}{V^S}) < V^{\max} < [\beta(d^E_{rl^{*\prime}} - \tilde{D}^{ES}_r)]/(T \cdot \tilde{q}_r - T_r - \frac{d^N_{rl^{*\prime}} - \tilde{D}^S_r}{V^{\max}} - \frac{\tilde{D}^{ES}_r + \tilde{D}^S_r}{V^S})$, so that when $\hat{q}^E_{rl^*} \le \tilde{q}_r < \hat{q}^E_{rl^{*\prime}}$, $g'(d^E_{rl^*}, d^N_{rl^*}, t^{E*}_r, t^{S*}_r, t^{ES*}_r, t^{N*}_r, \tilde{q}_r, \tilde{y}_r) < g'(d^E_{rl^{*\prime}}, d^N_{rl^{*\prime}}, t^{E*}_r, t^{S*}_r, t^{ES*}_r, t^{N*}_r, \tilde{q}_r, \tilde{y}_r)$ based on the result in (iii).

(v) When $q^{\min}_{rl^*} \le \tilde{q}_r < \hat{q}^E_{rl^*}$, we consider a new super path $l''$ that satisfies $d^E_{rl''} + d^N_{rl''} = d^E_{rl^{*\prime}} + d^N_{rl^{*\prime}} < d^E_{rl^*} + d^N_{rl^*}$ and $d^E_{rl''} = d^E_{rl^*} < d^E_{rl^{*\prime}}$. A new function $G(x) = (x - \tilde{D}^{ES}_r)^{b+1}a(T \cdot \tilde{q}_r - T_r - \frac{d^E_{rl^{*\prime}} + d^N_{rl^{*\prime}} - x - \tilde{D}^S_r}{V^{\max}} - \frac{\tilde{D}^{ES}_r + \tilde{D}^S_r}{V^S})^{-b} + \tilde{D}^{ES}_r \cdot a(V^S)^b + (d^E_{rl^{*\prime}} + d^N_{rl^{*\prime}} - x - \tilde{D}^S_r) \cdot a(V^{\max})^b + \tilde{D}^S_r \cdot a(V^S)^b$ is presented with the first-order derivative $\frac{dG(x)}{dx} = a(b+1)(x - \tilde{D}^{ES}_r)^b(T \cdot \tilde{q}_r - T_r - \frac{d^E_{rl^{*\prime}} + d^N_{rl^{*\prime}} - x - \tilde{D}^S_r}{V^{\max}} - \frac{\tilde{D}^{ES}_r + \tilde{D}^S_r}{V^S})^{-b} - ab\frac{1}{V^{\max}}(x - \tilde{D}^{ES}_r)^{b+1}(T \cdot \tilde{q}_r - T_r - \frac{d^E_{rl^{*\prime}} + d^N_{rl^{*\prime}} - x - \tilde{D}^S_r}{V^{\max}} - \frac{\tilde{D}^{ES}_r + \tilde{D}^S_r}{V^S})^{-(b+1)} - a(V^{\max})^b$. We derive that $\frac{dG(x)}{dx} = 0$ when $\tilde{q}_r = [(d^E_{rl^{*\prime}} - \tilde{D}^{ES}_r)V^S + (d^N_{rl^{*\prime}} - \tilde{D}^S_r)V^S + T_r V^{\max} V^S + (\tilde{D}^{ES}_r + \tilde{D}^S_r)V^{\max}]/(T \cdot V^{\max} V^S) \le q^{\min}_{rl^{*\prime}}$ and $\frac{dG(x)}{dx}$ decreases with the increase of $\tilde{q}_r$, and thus $\frac{dG(x)}{dx} < 0$ when $q^{\min}_{rl^*} \le \tilde{q}_r < \hat{q}^E_{rl^*}$. According to the function $G(x)$, we have $g(d^E_{rl^*}, d^N_{rl^*}, t^{E*}_r, t^{S*}_r, t^{ES*}_r, t^{N*}_r, \tilde{q}_r, \tilde{y}_r) > g'(d^E_{rl^*}, d^N_{rl^*}, t^{E*}_r, t^{S*}_r, t^{ES*}_r, t^{N*}_r, \tilde{q}_r, \tilde{y}_r) + c^{CO_2} \cdot G(d^E_{rl''}) > g'(d^E_{rl^{*\prime}}, d^N_{rl^{*\prime}}, t^{E*}_r, t^{S*}_r, t^{ES*}_r, t^{N*}_r, \tilde{q}_r, \tilde{y}_r) + c^{CO_2} \cdot G(d^E_{rl^{*\prime}}) = g(d^E_{rl^{*\prime}}, d^N_{rl^{*\prime}}, t^{E*}_r, t^{S*}_r, t^{ES*}_r, t^{N*}_r, \tilde{q}_r, \tilde{y}_r)$.

Based on the results of all cases, we can draw a conclusion that $d^E_{rl^*} + d^N_{rl^*}$ must be shorter than or equal to $d^E_{rl^{*\prime}} + d^N_{rl^{*\prime}}$. $\square$

## Appendix E. Proof of Proposition 6

*Proof.* In this proposition, we assume that $q_r$ can take fractional quantities. When $q_r^{\text{MIN}} \leq q_r < \hat{q}_r^{S,\max}$, the change of compliance of VSRZs is one reason for the non-convex property of the total cost function (23), which can be explained by the following example. Consider a route $r$ with only one VSRZ port $p$ covering a 20 nm VSRZ (recorded as VSRZ 1) and several ECA and non-ES ports, and it has only one super path $l$ whose sailing distances within and outside ECAs are $d_{rl}^E = 800$ and $d_{rl}^N = 18,000$. The parameters in the example are set as follows: $a = 0.00047$, $b = 2.118$, $\alpha^E = 600$, $\alpha^N = 500$, $c^{CO_2} = 76$, $c^{fix} = 387,000$, $c_{rp1}^{ref} = 1,000$, $V^{\max} = 25$, and $T_r = 0$. When 6 ships are deployed on the route, by optimizing the sailing speeds, the total costs before and after participating in the VSRZ are 4,839,952 USD and 4,842,023 USD, respectively; when 7 ships are deployed, the total costs are 4,525,578 USD and 4,525,553 USD. Therefore, the minimum total cost can be obtained by not participating in the VSRZ first and then participating in the VSRZ with the increase of the number of ships deployed, and the minimum total cost function (denoted by $C_r^{\min}(q_r)$) is non-convex shown in the thick solid line of Fig. E.8.

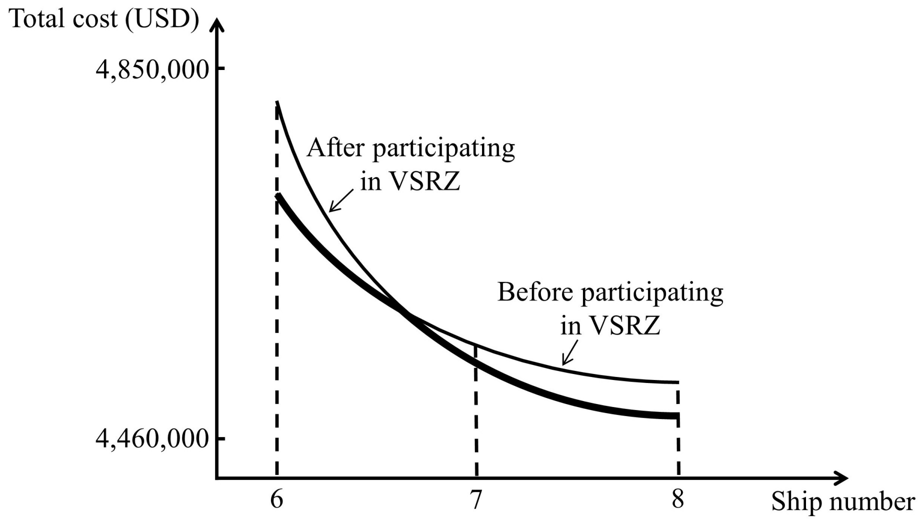


Figure E.8: Total cost curves

When $q_r \geq \hat{q}_r^{S,\max}$, super path $l^*$ with the minimum $\beta d_{rl^*}^E + d_{rl^*}^N$ will always be chosen and all VSRIPs will be obeyed according to Propositions 2 and 4. Hence, the total cost function is $(\alpha^N + c^{CO_2})(\beta d_{rl^*}^E + d_{rl^*}^N)^{b+1} \cdot a(T \cdot q_r - T_r)^{-b} - \sum_{p \in P_r^S \cup P_r^{ES}} c_{rp|J_{rp}|}^{ref} + c^{fix} q_r$, whose second-order derivative is $(\alpha^N + c^{CO_2})(\beta d_{rl^*}^E + d_{rl^*}^N)^{b+1} \cdot ab(b+1)T^2(T \cdot q_r - T_r)^{-(b+2)} > 0$, meaning that the function is convex with the increase of $q_r$. $\square$

## Appendix F. Proof of Proposition 7

*Proof.* When $\sum_{r\in R} q_r^* > Q$, the dynamic programming algorithm is employed to address the fleet deployment problem. We analyze each feasible decision $q_r = q_r^{\mathrm{MIN}}, ..., \min\{q_r^*, Q - \sum_{r'\in R\setminus\{r\}} q_{r'}^{\mathrm{MIN}}\}$ in each state $Q_r = \sum_{r'=1}^{r} q_{r'}^{\mathrm{MIN}}, ..., \min\{\sum_{r'=1}^{r} q_{r'}^*, Q - \sum_{r'=r+1}^{|R|} q_{r'}^{\mathrm{MIN}}\}$ for each route $r \in R$, and hence both the numbers of feasible decisions $q_r$ and states $Q_r$ do not exceed $Q$. We assume that the values of $C_r^{\min}(q_r)$ for all $r \in R$ and $q_r = q_r^{\mathrm{MIN}}, ..., \min\{q_r^*, Q - \sum_{r'\in R\setminus\{r\}} q_{r'}^{\mathrm{MIN}}\}$ are given. We conclude that when $\sum_{r\in R} q_r^* > Q$, the computational time for the fleet deployment problem is bounded by $O\left(|R| \cdot Q^2\right)$. $\square$


## Acknowledgments

This work was supported by the National Natural Science Foundation of China [Grant Nos. 72071173, 71831008] and the Research Grants Council of the Hong Kong Special Administrative Region, China [Project number 15200817].


## References


Adland, R., Fonnes, G., Jia, H., Lampe, O.D., Strandenes, S.P., 2017. The impact of regional environmental regulations on empirical vessel speeds. Transportation Research Part D: Transport and Environment 53, 37–49.

Ahl, C., Frey, E., Steimetz, S., 2017. The effects of financial incentives on vessel speed reduction: Evidence from the Port of Long Beach green flag incentive program. Maritime Economics & Logistics 19, 601–618.

Andersson, H., Fagerholt, K., Hobbesland, K., 2015. Integrated maritime fleet deployment and speed optimization: Case study from RoRo shipping. Computers & Operations Research 55, 233–240.

Browning, L., Hartley, S., Bandemehr, A., Gathright, K., Miller, W., 2012. Demonstration of fuel switching on oceangoing vessels in the Gulf of Mexico. Journal of the Air & Waste Management Association 62, 1093–1101.

Cariou, P., Cheaitou, A., Larbi, R., Hamdan, S., 2018. Liner shipping network design with emission control areas: A genetic algorithm-based approach. Transportation Research Part D: Transport and Environment 63, 604–621.

Chang, C.C., Jhang, C.W., 2016. Reducing speed and fuel transfer of the green flag incentive program in Kaohsiung Port Taiwan. Transportation Research Part D: Transport and Environment 46, 1–10.

Chang, C.C., Wang, C.M., 2014. Evaluating the effects of speed reduce for shipping costs and $CO_2$ emission. Transportation Research Part D: Transport and Environment 31, 110–115.

Chang, Y.T., Roh, Y., Park, H., 2014. Assessing noxious gases of vessel operations in a potential emission control area. Transportation Research Part D: Transport and Environment 28, 91–97.

Chen, L., Yip, T.L., Mou, J., 2018. Provision of emission control area and the impact on shipping route choice and ship emissions. Transportation Research Part D: Transport and Environment 58, 280–291.

Corbett, J.J., Wang, H., Winebrake, J.J., 2009. The effectiveness and costs of speed reductions on emissions from international shipping. Transportation Research Part D: Transport and Environment 14, 593–598.

Cullinane, S., Edwards, J., 2010. Assessing the environmental impacts of freight transport. Green Logistics: Improving the Environmental Sustainability of Logistics , 31–48.

Dong, B., Christiansen, M., Fagerholt, K., Bektaş, T., 2020a. Combined maritime fleet deployment and inventory management with port visit flexibility in roll-on roll-off shipping. Transportation Research Part E: Logistics and Transportation Review 140, 101988.

Dong, B., Christiansen, M., Fagerholt, K., Chandra, S., 2020b. Design of a sustainable maritime multi-modal distribution network–Case study from automotive logistics. Transportation Research Part E: Logistics and Transportation Review 143, 102086.

Doudnikoff, M., Lacoste, R., 2014. Effect of a speed reduction of containerships in response to higher energy costs in sulphur emission control areas. Transportation Research Part D: Transport and Environment 28, 51–61.

Fagerholt, K., Gausel, N.T., Rakke, J.G., Psaraftis, H.N., 2015. Maritime routing and speed optimization with emission control areas. Transportation Research Part C: Emerging Technologies 52, 57–73.

Fagerholt, K., Psaraftis, H.N., 2015. On two speed optimization problems for ships that sail in and out of emission control areas. Transportation Research Part D: Transport and Environment 39, 56–64.

Fan, L., Huang, L., 2019. Analysis of the incentive for slow steaming in Chinese sulfur emission control areas. Transportation Research Record 2673, 165–175.

Gu, Y., Wallace, S.W., 2017. Scrubber: A potentially overestimated compliance method for the emission control areas: The importance of involving a ship's sailing pattern in the evaluation. Transportation Research Part D: Transport and Environment 55, 51–66.

ICE, 2020. EUA price. URL: https://www.theice.com/products/197/EUA-Futures/data?marketId=6286683&span=1. (Accessed on 14 April 2020).

IMO, 2014. Third IMO GHG Study 2014: Executive Summary and Final Report. International Maritime Organization, London, UK. URL: http://www.imo.org/en/OurWork/Environment/PollutionPrevention/AirPollution/Documents/Third%20Greenhouse%20Gas%20Study/GHG3%20Executive%20Summary%20and%20Report.pdf. (Accessed on 25 March 2020).

Karsten, C.V., Ropke, S., Pisinger, D., 2018. Simultaneous optimization of container ship sailing speed and container routing with transit time restrictions. Transportation Science 52, 769–787.

Khan, M.Y., Agrawal, H., Ranganathan, S., Welch, W.A., Miller, J.W., Cocker III, D.R., 2012. Greenhouse gas and criteria emission benefits through reduction of vessel speed at sea. Environmental Science & Technology 46, 12600–12607.

Kim, H.J., Chang, Y.T., Kim, K.T., Kim, H.J., 2012. An epsilon-optimal algorithm considering greenhouse gas emissions for the management of a ship's bunker fuel. Transportation Research Part D: Transport and Environment 17, 97–103.

Kirschstein, T., Meisel, F., 2015. GHG-emission models for assessing the eco-friendliness of road and rail freight transports. Transportation Research Part B: Methodological 73, 13–33.

Koza, D.F., 2019. Liner shipping service scheduling and cargo allocation. European Journal of Operational Research 275, 897–915.

Li, L., Gao, S., Yang, W., Xiong, X., 2020. Ship's response strategy to emission control areas: From the perspective of sailing pattern optimization and evasion strategy selection. Transportation Research Part E: Logistics and Transportation Review 133, 101835.

Lloyd's List, 2020. EU votes to include shipping in emissions trading system. URL: https://lloydslist.maritimeintelligence.informa.com/LL1133898/EU-votes-to-include-shipping-in-Emissions-Trading-System. (Accessed on 25 October 2020).

López-Aparicio, S., Tønnesen, D., Thanh, T.N., Neilson, H., 2017. Shipping emissions in a Nordic Port: Assessment of mitigation strategies. Transportation Research Part D: Transport and Environment 53, 205–216.

Ma, D., Ma, W., Jin, S., Ma, X., 2020a. Method for simultaneously optimizing ship route and speed with emission control areas. Ocean Engineering 202, 107170.

Ma, W., Lu, T., Ma, D., Wang, D., Qu, F., 2020b. Ship route and speed multi-objective optimization considering weather conditions and emission control area regulations. Maritime Policy & Management, in press.

Meng, Q., Wang, S., Andersson, H., Thun, K., 2014. Containership routing and scheduling in liner shipping: Overview and future research directions. Transportation Science 48, 265–280.

Ng, M., 2019. Vessel speed optimisation in container shipping: A new look. Journal of the Operational Research Society 70, 541–547.

Ng, M., Lin, D.Y., 2018. Fleet deployment in liner shipping with incomplete demand information. Transportation Research Part E: Logistics and Transportation Review 116, 184–189.

Qi, X., Song, D.P., 2012. Minimizing fuel emissions by optimizing vessel schedules in liner shipping with uncertain port times. Transportation Research Part E: Logistics and Transportation Review 48, 863–880.

Reinhardt, L.B., Pisinger, D., Sigurd, M.M., Ahmt, J., 2020. Speed optimizations for liner networks with business constraints. European Journal of Operational Research 285, 1127–1140.

Sheng, D., Li, Z.C., Fu, X., Gillen, D., 2017. Modeling the effects of unilateral and uniform emission regulations under shipping company and port competition. Transportation Research Part E: Logistics and Transportation Review 101, 99–114.

Sheng, D., Meng, Q., Li, Z.C., 2019. Optimal vessel speed and fleet size for industrial shipping services under the emission control area regulation. Transportation Research Part C: Emerging Technologies 105, 37–53.

Shin, S.H., Lee, P.T.W., Lee, S.W., 2019. Lessons from bankruptcy of Hanjin Shipping Company in chartering. Maritime Policy & Management 46, 136–155.

Ship and Bunker, 2020. World bunker prices. URL: https://shipandbunker.com/prices. (Accessed on 14 April 2020).

Sofiev, M., Winebrake, J.J., Johansson, L., Carr, E.W., Prank, M., Soares, J., Vira, J., Kouznetsov, R., Jalkanen, J.P., Corbett, J.J., 2018. Cleaner fuels for ships provide public health benefits with climate tradeoffs. Nature Communications 9, 1–12.

Svindland, M., 2018. The environmental effects of emission control area regulations on short sea shipping in Northern Europe: The case of container feeder vessels. Transportation Research Part D: Transport and Environment 61, 423–430.

Tan, Z., Wang, Y., Meng, Q., Liu, Z., 2018. Joint ship schedule design and sailing speed optimization for a single inland shipping service with uncertain dam transit time. Transportation Science 52, 1570–1588.

UNCTAD, 2019. Review of Maritime Transportation 2019. Paper presented at the United Nations Conference on Trade and Development, New York and Geneva. URL: http://unctad.org/en/PublicationsLibrary/rmt2019_en.pdf. (Accessed on 25 March 2020).

Wang, C., Chen, J., 2017. Strategies of refueling, sailing speed and ship deployment of containerships in the low-carbon background. Computers & Industrial Engineering 114, 142–150.

Wang, C., Xu, C., 2015. Sailing speed optimization in voyage chartering ship considering different carbon emissions taxation. Computers & Industrial Engineering 89, 108–115.

Wang, S., Gao, S., Tan, T., Yang, W., 2019. Bunker fuel cost and freight revenue optimization for a single liner shipping service. Computers & Operations Research 111, 67–83.

Wang, S., Meng, Q., 2012. Sailing speed optimization for container ships in a liner shipping network. Transportation Research Part E: Logistics and Transportation Review 48, 701–714.

Wang, S., Meng, Q., 2017. Container liner fleet deployment: A systematic overview. Transportation Research Part C: Emerging Technologies 77, 389–404.

Xin, X., Wang, X., Tian, X., Chen, Z., Chen, K., 2019. Green scheduling model of shuttle tanker fleet considering carbon tax and variable speed factor. Journal of Cleaner Production 234, 1134–1143.

Zhang, Q., Zheng, Z., Wan, Z., Zheng, S., 2020. Does emission control area policy reduce sulfur dioxides concentration in Shanghai? Transportation Research Part D: Transport and Environment 81, 102289.

Zhao, Y., Fan, Y., Zhou, J., Kuang, H., 2019. Bi-objective optimization of vessel speed and route for sustainable coastal shipping under the regulations of emission control areas. Sustainability 11, 6281.

Zhen, L., Hu, Y., Wang, S., Laporte, G., Wu, Y., 2019. Fleet deployment and demand fulfillment for container shipping liners. Transportation Research Part B: Methodological 120, 15–32.

Zhen, L., Hu, Z., Yan, R., Zhuge, D., Wang, S., 2020a. Route and speed optimization for liner ships under emission control policies. Transportation Research Part C: Emerging Technologies 110, 330–345.

Zhen, L., Li, M., Hu, Z., Lv, W., Zhao, X., 2018. The effects of emission control area regulations on cruise shipping. Transportation Research Part D: Transport and Environment 62, 47–63.

Zhen, L., Wu, Y., Wang, S., Laporte, G., 2020b. Green technology adoption for fleet deployment in a shipping network. Transportation Research Part B: Methodological 139, 388–410.

Zhuge, D., Wang, S., Zhen, L., Laporte, G., 2020. Schedule design for liner services under vessel speed reduction incentive programs. Naval Research Logistics 67, 45–62.

Zis, T., 2015. The Implications and Trade-Offs of Near-Port Ship Emissions Reduction Policies. Ph.D. thesis. Imperial College London.

Zis, T., North, R.J., Angeloudis, P., Ochieng, W.Y., Bell, M.G.H., 2014. Evaluation of cold ironing and speed reduction policies to reduce ship emissions near and at ports. Maritime Economics & Logistics 16, 371–398.

Zis, T., Psaraftis, H.N., Ding, L., 2020. Ship weather routing: A taxonomy and survey. Ocean Engineering 213, 107697.